

Full-Scale S-76 Rotor Performance and Loads at Low Speeds in the NASA Ames 80- by 120-Foot Wind Tunnel

Volume 1

Patrick M. Shinoda, *Aeroflightdynamics Directorate, U.S. Army Aviation and Troop Command, Ames Research Center, Moffett Field, California*

April 1996



National Aeronautics and Space Administration

Ames Research Center
Moffett Field, CA 94035-1000



US Army
Aviation and Troop Command

Aeroflightdynamics Directorate
Moffett Field, CA 94035-1000

Full-Scale S-76 Rotor Performance and Loads at Low Speeds in the NASA Ames 80- by 120-Foot Wind Tunnel

Volume 1

Patrick M. Shinoda

April 1996



National Aeronautics and
Space Administration



US Army
Aviation and Troop Command

Table 1. General characteristics of the S-76 main rotor

Parameter	Value
Radius	22 ft
Nominal Chord	15.5 in
Nominal twist	-10 deg
Blade Reference Area	113.67 ft ²
Solidity Ratio	.0748
Number of Blades	4
Airfoils	SC1095 84% outboard SC1095R8 80% inboard
Flapping Hinge offset	3.70% radius
Lock No.	11.6
100% RPM	293
100% tip speed	675 fps

Table 2. RTA Rotor balance capabilities and static load accuracies at the balance moment center

Measurement Parameters	Measured Standard Deviation of Error		
	Maximum Capacity	Value	% Capacity
Normal Force or Lift (NF), lb	22,000	25	0.12
Side Force (SF), lb	4,400	7	0.16
Axial Force or Drag (AF), lb	4,400	12	0.27
Pitching Moment (PM), ft-lb	57,833	27	0.05
Rolling Moment (RM), ft-lb	57,833	42	0.07
Torque(TQ), ft-lb	36,083	--	--

Table 3. Aero tare coefficient matrix

$$\text{Aero Load} = C_0 + C_1 * QPSF + C_2 * QPSF^2$$

ALFS,U	Balance Parameter	C0	C1	C2
-15°	NF	0.000000E+00	-0.326101E+01	0.476469E-01
	AF	0.000000E+00	0.661349E+01	0.143181E-02
	SF	0.000000E+00	0.000000E+00	0.000000E+00
	PM	0.000000E+00	0.370070E+02	-0.296749E-01
	RM	0.000000E+00	-0.896100E+00	0.971002E-02
	TQ	0.106000E+03	0.194928E+01	-0.21002E-01
-10°	NF	0.000000E+00	-0.298026E+01	0.584926E-01
	AF	0.000000E+00	0.684417E+01	-0.163840E-01
	SF	0.000000E+00	-0.384309E+00	0.145089E-02
	PM	0.000000E+00	0.352023E+02	-0.256171E-01
	RM	0.000000E+00	-0.562534E+00	0.181376E-02
	TQ	0.106000E+03	0.274941E+01	-0.382801E-01
-5°	NF	0.000000E+00	0.000000E+00	0.000000E+00
	AF	0.000000E+00	0.000000E+00	0.000000E+00
	SF	0.000000E+00	-0.986075E+00	0.290571E-01
	PM	0.000000E+00	0.366249E+02	-0.117064E-01
	RM	0.000000E+00	-0.130419E+01	0.172222E-01
	TQ	0.106000E+03	0.181556E+01	-0.185694E-01
-2°	NF	0.000000E+00	-0.371327E+01	0.116512E+00
	AF	0.000000E+00	0.616055E+01	-0.157009E-01
	SF	0.000000E+00	-0.107114E+01	0.182306E-01
	PM	0.000000E+00	0.356245E+02	-0.376357E-01
	RM	0.000000E+00	-0.102194E+01	0.266390E-01
	TQ	0.106000E+03	-0.194027E+01	-0.119433E-01
0°	NF	0.000000E+00	0.314353E+01	-0.662631E-01
	AF	0.000000E+00	0.590607E+01	0.324471E-02
	SF	0.000000E+00	-0.857955E+00	0.107120E-02
	PM	0.000000E+00	0.353893E+02	-0.353695E-01
	RM	0.000000E+00	-0.135617E+01	0.175815E-01
	TQ	0.106000E+03	0.249418E+01	-0.338657E-01
+5°	NF	0.000000E+00	0.184863E+00	0.969723E-02
	AF	0.000000E+00	0.625300E+01	-0.188129E-01
	SF	0.000000E+00	-0.106543E+01	0.135065E-01
	PM	0.000000E+00	0.354519E+02	-0.399007E-01
	RM	0.000000E+00	-0.236734E+01	0.514371E-01
	TQ	0.106000E+03	0.166225E+01	-0.607216E-03

Table 3. Aero tare coefficient matrix (continued)

$$\text{Aero Load} = C_0 + C_1 * QPSF + C_2 * QPSF^2$$

ALFS,U	Balance Parameter	C0	C1	C2
+10°	NF	0.000000E+00	0.222560E+01	-0.237747E-02
	AF	0.000000E+00	0.535671E+01	0.777188E-02
	SF	0.000000E+00	-0.114855E+01	0.166964E-01
	PM	0.000000E+00	0.344327E+02	-0.295324E-01
	RM	0.000000E+00	-0.139549E+01	0.491692E-02
	TQ	0.106000E+03	0.279907E+01	-0.351700E-01

Table 4. Fixed system measurements

Measurement	Location	Units	Sign Convention
Lift (NF)	Rotor Balance	lb	up
Side (SF)	Rotor Balance	lb	right
Drag (AF)	Rotor Balance	lb	aft
Pitch (PM)	Rotor Balance	ft-lb	nose up
Roll (RM)	Rotor Balance	ft-lb	right wing down

Table 5. Rotating system measurements

Measurement	Blade Number	Location (r/R)	Units	Sign Convention
Flap Bending	1	0.127	ft-lb	tip up
Flap Bending	1	0.200	ft-lb	tip up
Flap Bending	1	0.300	ft-lb	tip up
Flap Bending	1	0.679	ft-lb	tip up
Flap Bending	1	0.920	ft-lb	tip up
Chord Bending	1	0.127	ft-lb	tip aft
Chord Bending	1	0.200	ft-lb	tip aft
Chord Bending	1	0.300	ft-lb	tip aft
Chord Bending	1	0.454	ft-lb	tip aft
Pitch Link	1	Pitch Horn	lb	tension
Flap Angle	1	Pitch Horn	deg	flap up
Rotor Shaft Torque (TQ)	-	center of balance	ft-lb	counter clockwise

Table 6. Hover test matrix

Shaft Angles, α_S	-15°, -10°, -5°, 0°, 5°, 10°, 15°*
C _T /σ	0.02 - 0.12
MTIP	0.605
YAW	0°, 90°*

*Note: For YAW = 90°, hover data taken only at $\alpha_S = +15^\circ$

Table 7. Thrust sweep test matrix

$$\begin{aligned} C_T/\sigma &= 0.03-0.125 \\ MTIP &: 0.605 \text{ (675 fps)} \end{aligned}$$

		α_S					
VKTS	μ	10°	5°	0°	-2°	-10°	-15°
20	0.050				X		
32	0.080			X			
40	0.100	X	X		X	X	X
50	0.125	X	X				
60	0.150	X	X		X	X	X
80	0.200	X	X		X	X	
100	0.250	X	X		X	X	X

Table 8. Speed sweep test matrix

$$\begin{aligned} VKTS &= 0-100 \text{ kt} \\ MTIP &: 0.605 \text{ (675 fps)} \end{aligned}$$

		Thrust, lb		
		8,000 (C _T /σ = .065)	9,850 (.080)	12,320 (.100)
α_S	10°		X	X
	5°	X	X	X
	0°		X	
	-2°	X	X	X
	-5°	X	X	
	-10°	X	X	X



Figure 2. S-76 Rotor System installed on Rotor Test Apparatus in the Ames 80- by 120-Foot Wind Tunnel Test Section

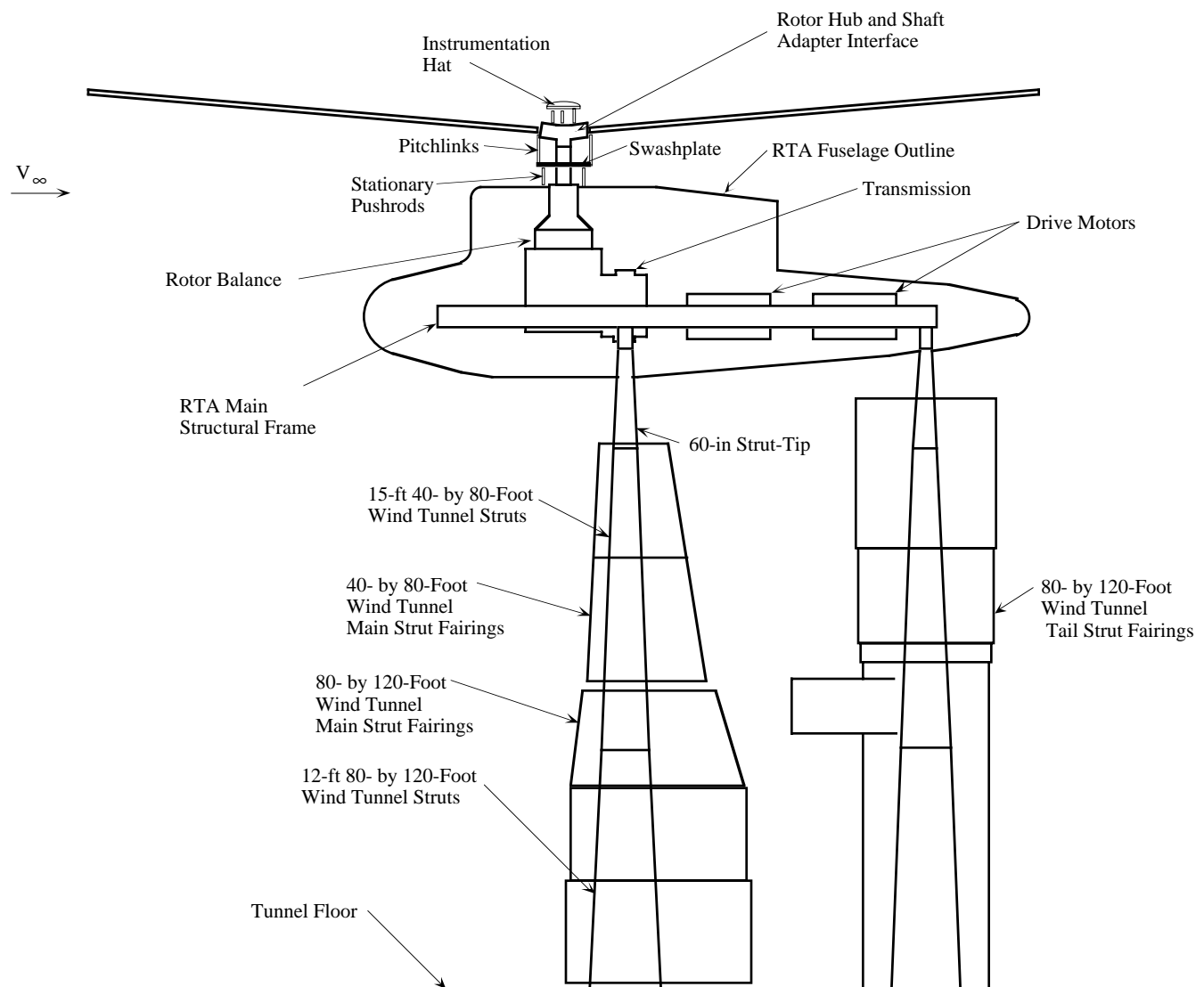


Figure 3(a). Schematic of RTA/S-76 rotor test set-up in the 80- by 120-Foot Wind Tunnel

Figure 3(b). Plan view of model in the 80- by 120-Foot Wind Tunnel test section YAW = 0 deg and 90 deg.

Figure 3(c). Sideview of model in tunnel test section $\alpha_S = 0 \text{ deg}, -15 \text{ deg}$ and 15 deg .

figure 4. Radial locations of blade flap and chord instrumentation for the wind tunnel test program.

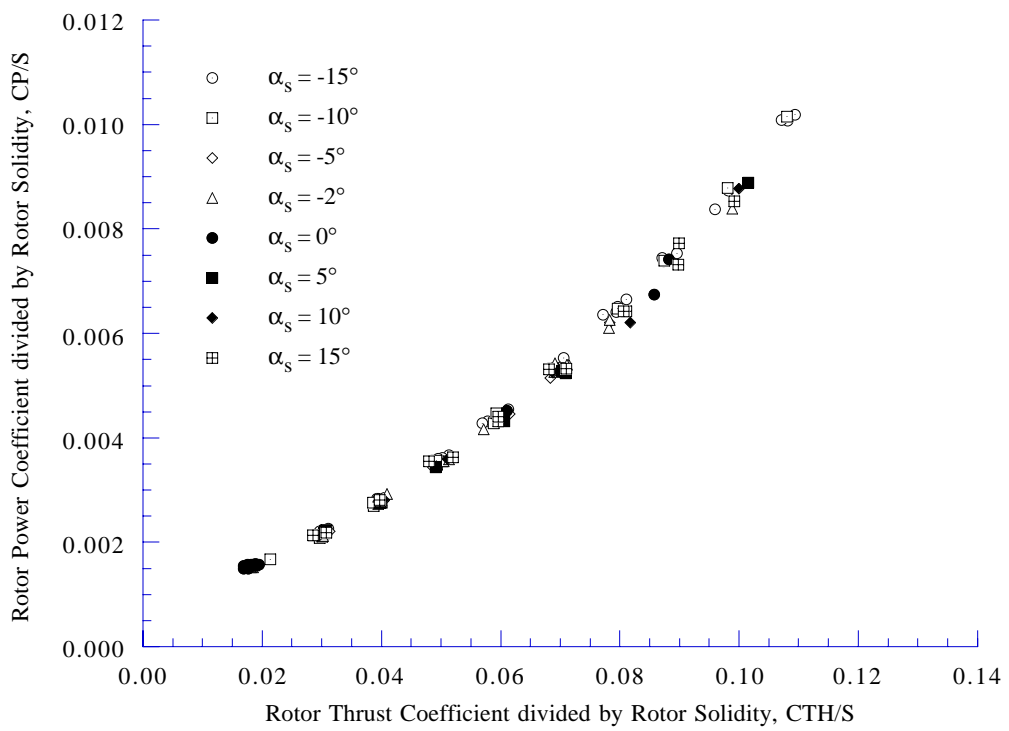


Figure 5(a). Rotor power coefficient as a function of rotor thrust coefficient, YAW = 0 deg, hover.

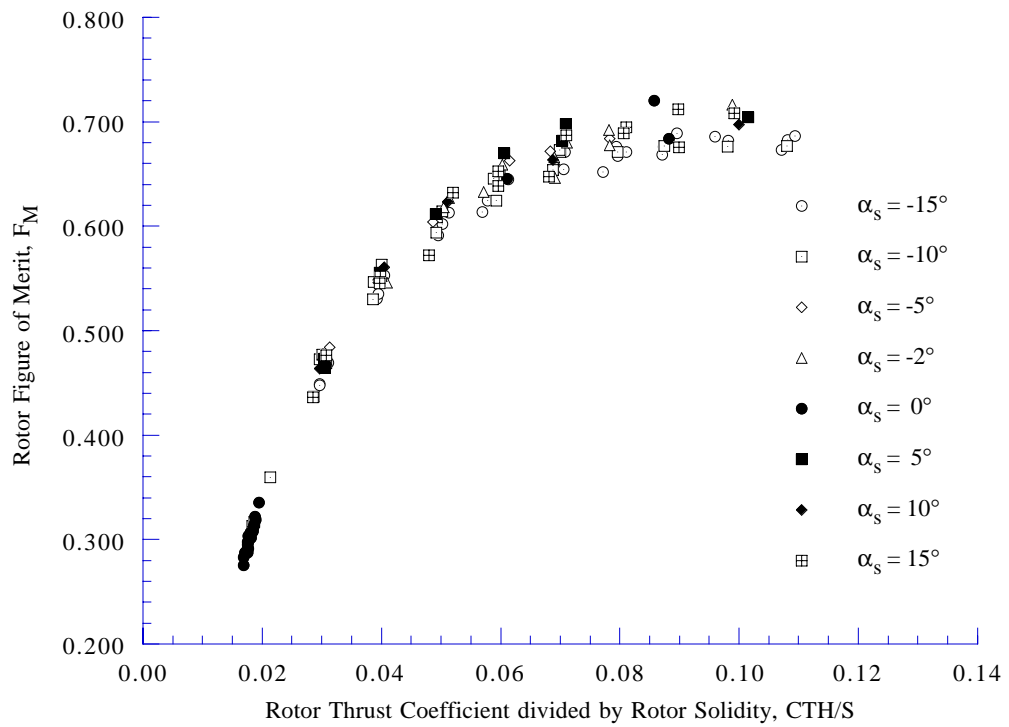


Figure 5(b). Rotor figure of merit as a function of rotor thrust coefficient, YAW = 0 deg, hover.

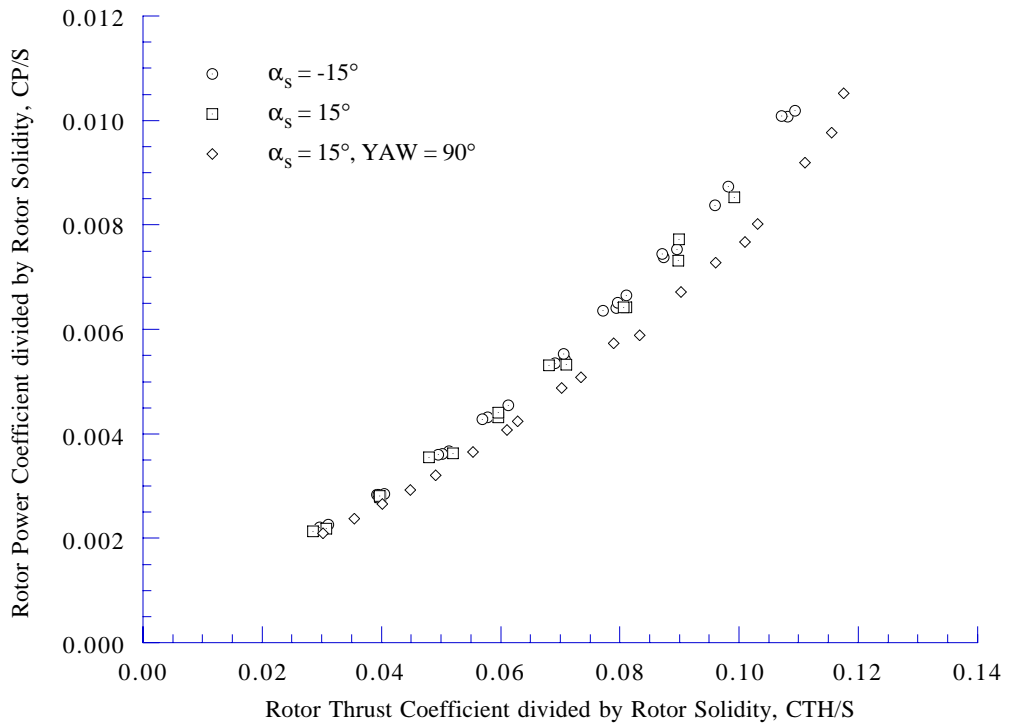


Figure 6(a). Rotor power coefficient as a function of rotor thrust coefficient at two different yaw positions, YAW = 0 deg, 90 deg, hover.

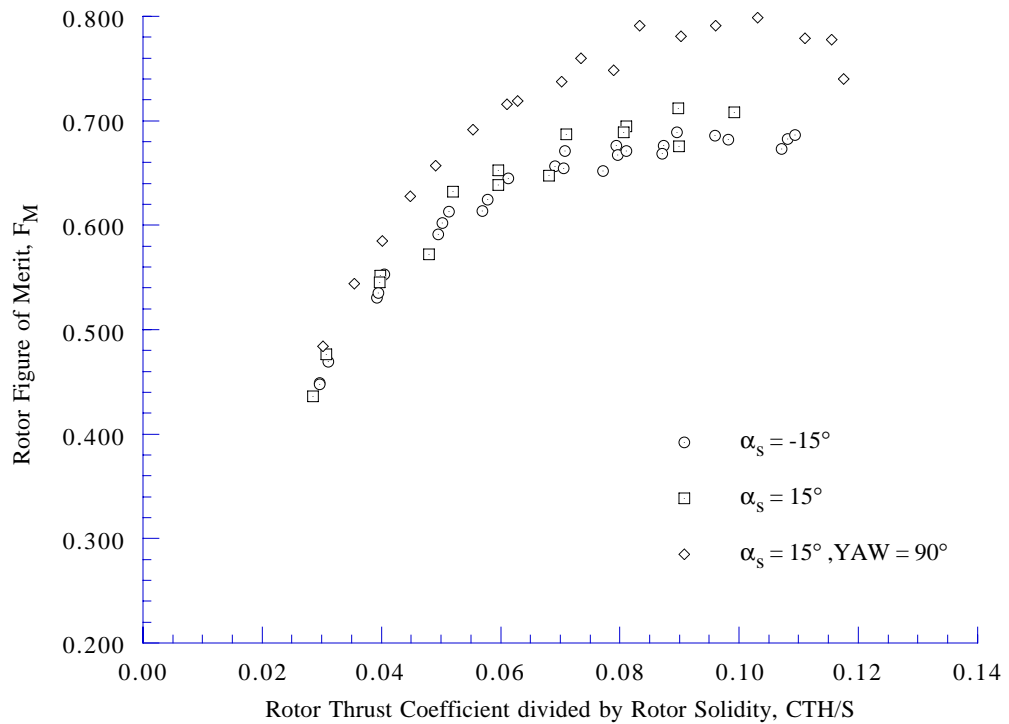


Figure 6(b). Rotor figure of merit as a function of rotor thrust coefficient at two different yaw positions, YAW = 0 deg, 90 deg, hover.

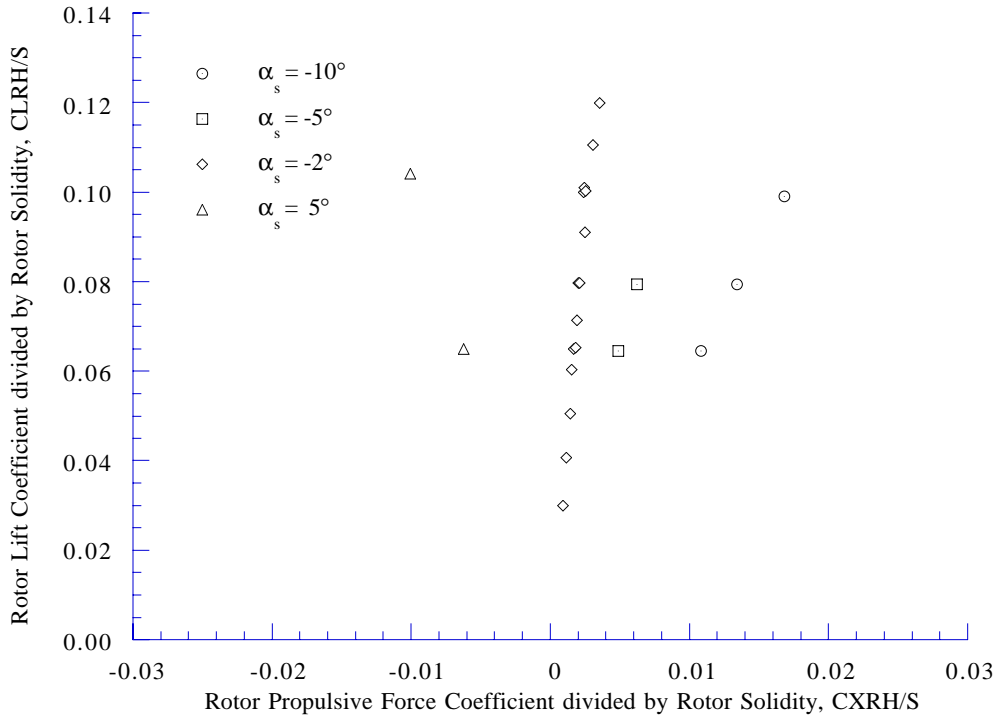


Figure 7(a). Rotor lift coefficient as a function of rotor propulsive force coefficient, 20 knots ($\mu = 0.05$).

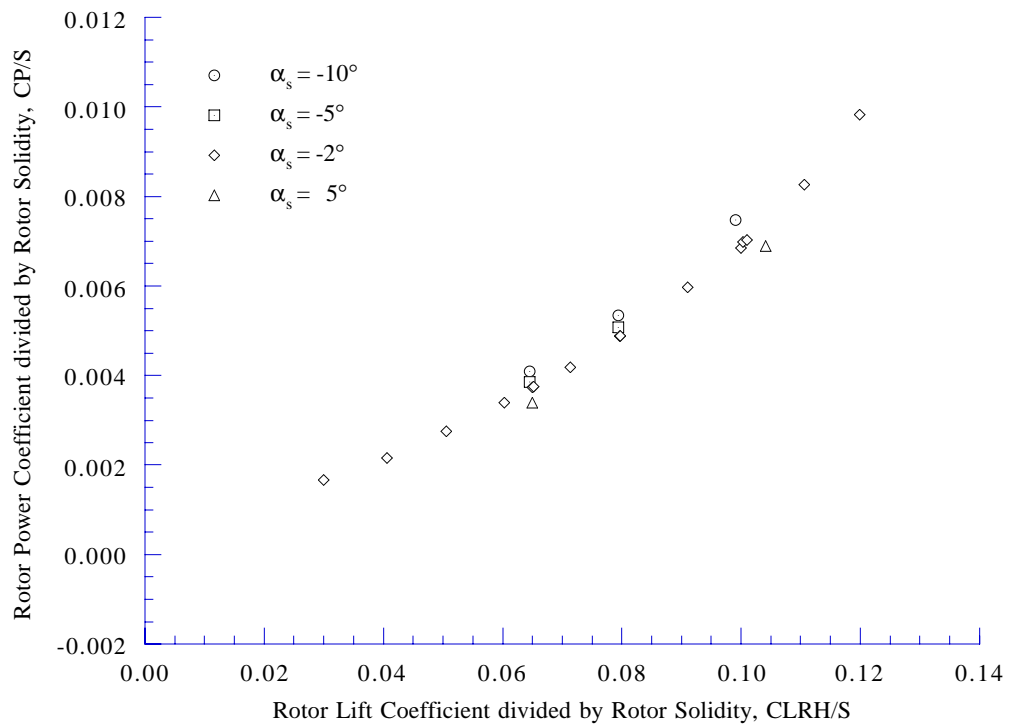


Figure 7(b). Rotor power coefficient as a function of rotor lift coefficient, 20 knots ($\mu = 0.05$).

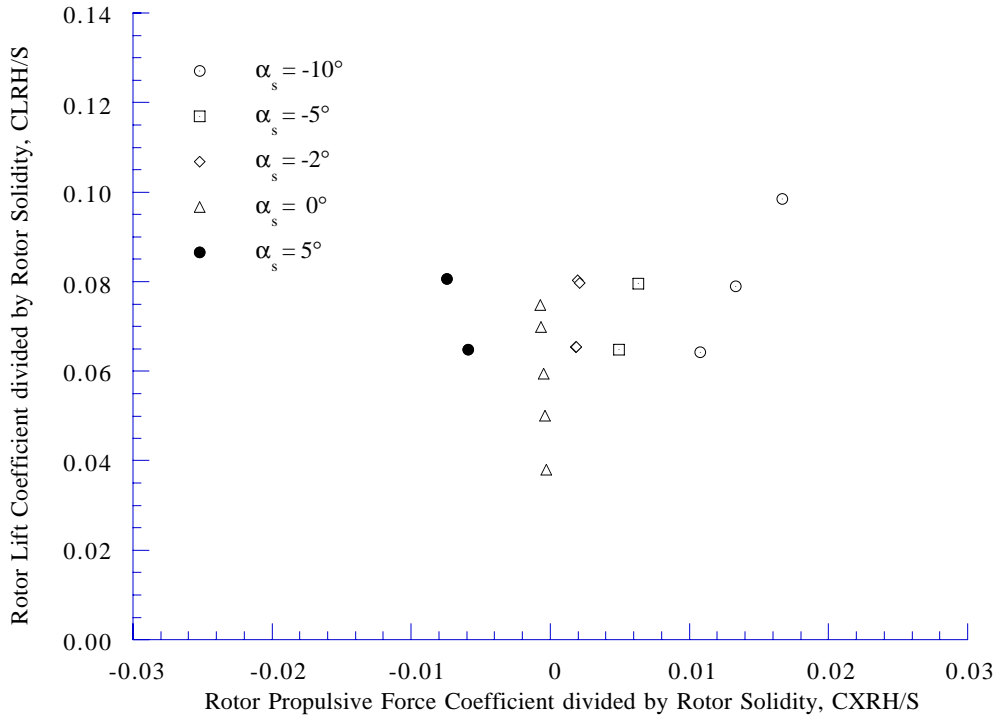


Figure 8(a). Rotor lift coefficient as a function of rotor propulsive force coefficient, 32 knots ($\mu = 0.08$).

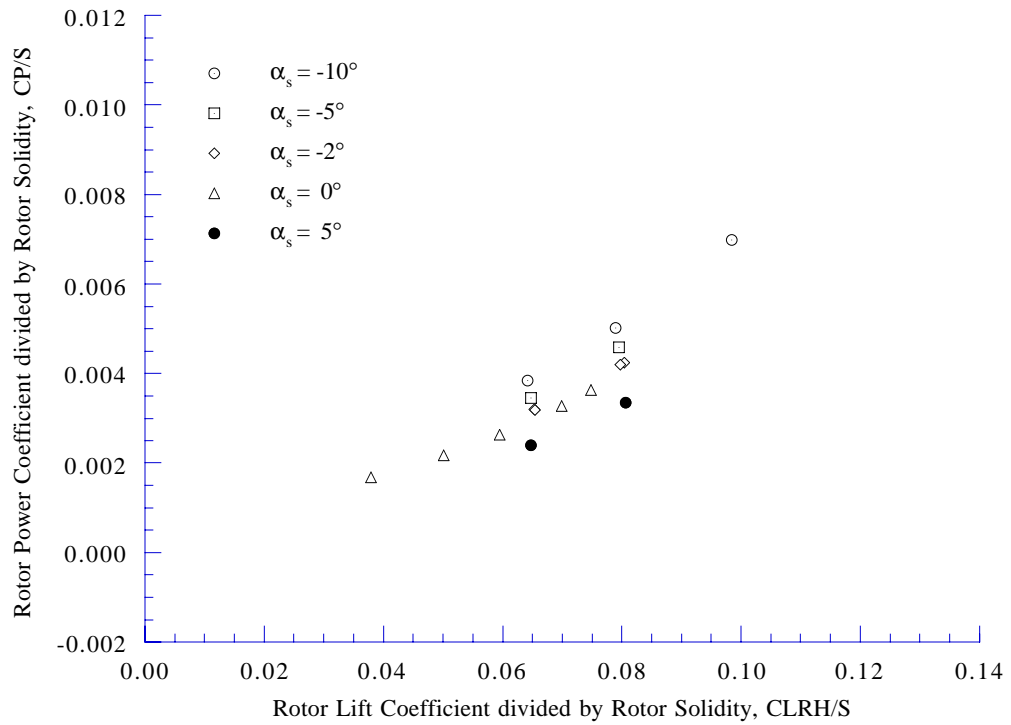


Figure 8(b). Rotor power coefficient as a function of rotor lift coefficient, 32 knots ($\mu = 0.08$).

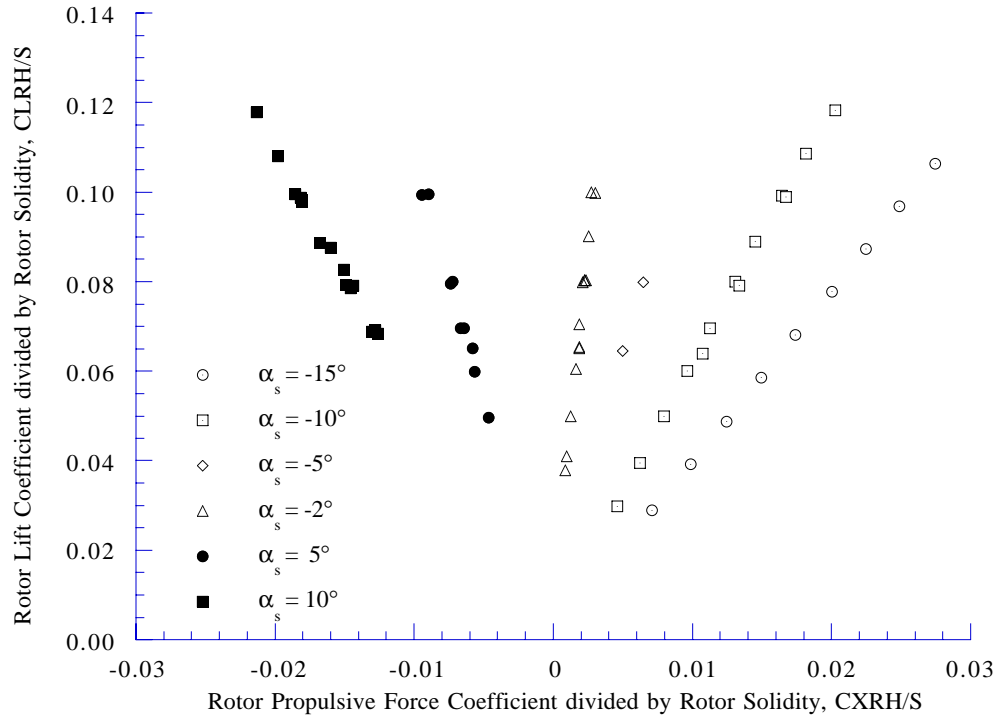


Figure 9(a). Rotor lift coefficient as a function of rotor propulsive force coefficient, 40 knots ($\mu = 0.10$).

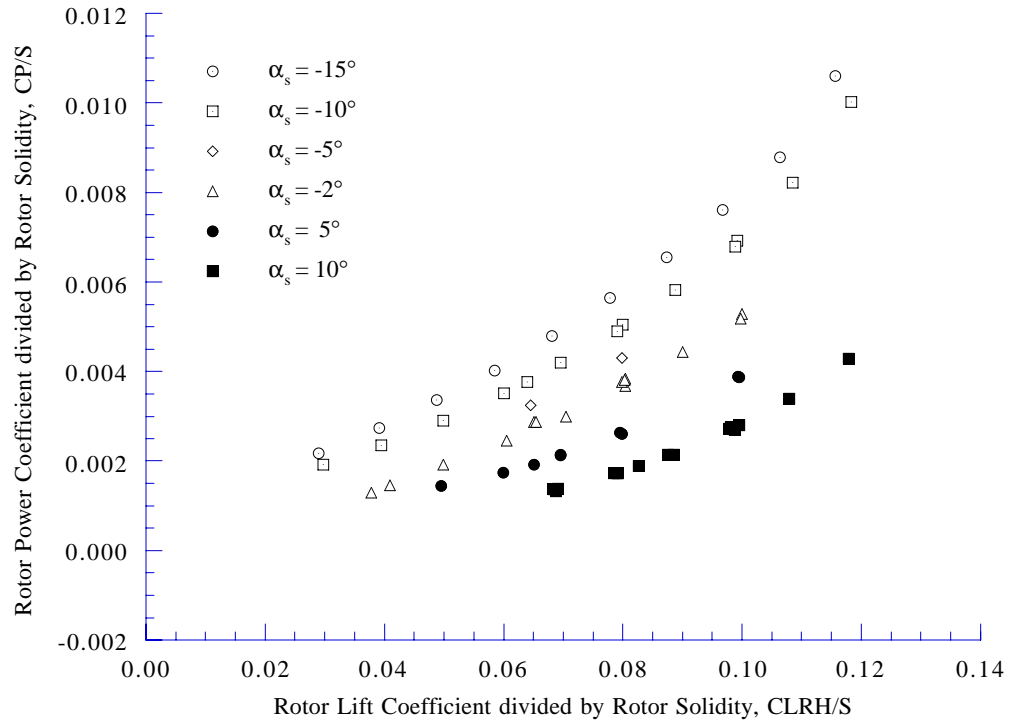


Figure 9(b). Rotor power coefficient as a function of rotor lift coefficient, 40 knots ($\mu = 0.10$).

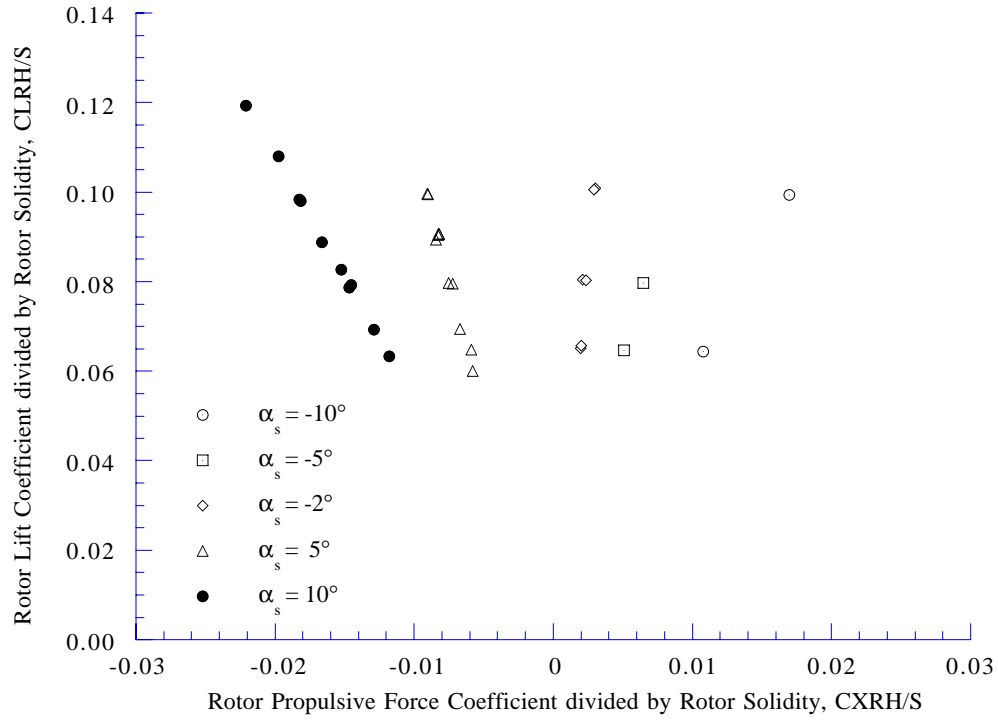


Figure 10(a). Rotor lift coefficient as a function of rotor propulsive force coefficient, 50 knots ($\mu = 0.125$).

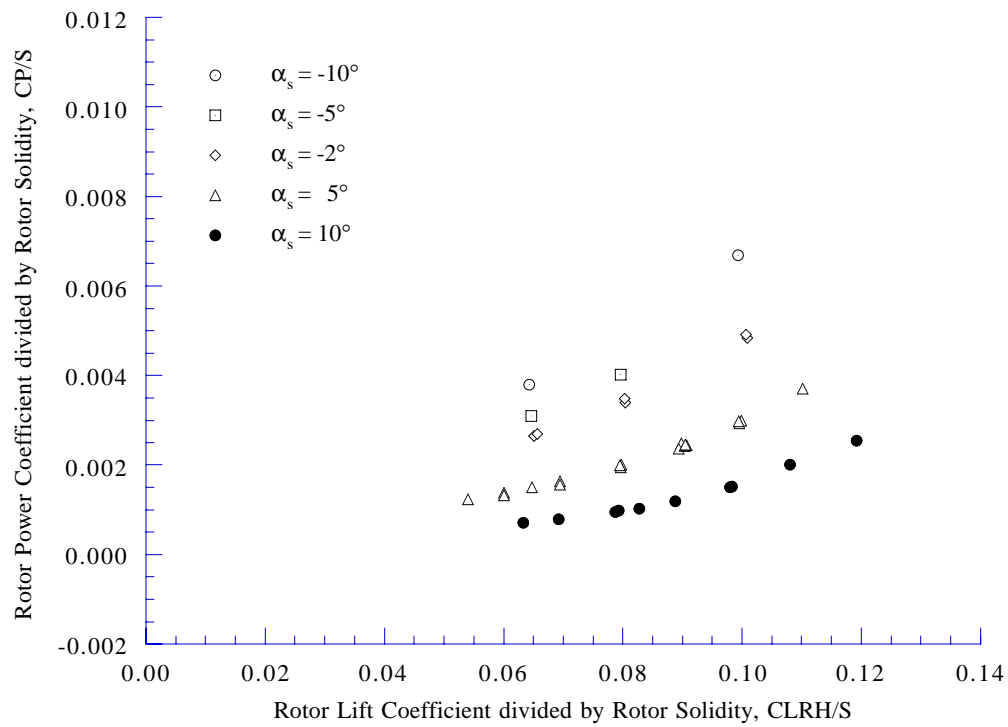


Figure 10(b). Rotor power coefficient as a function of rotor lift coefficient, 50 knots ($\mu = 0.125$).

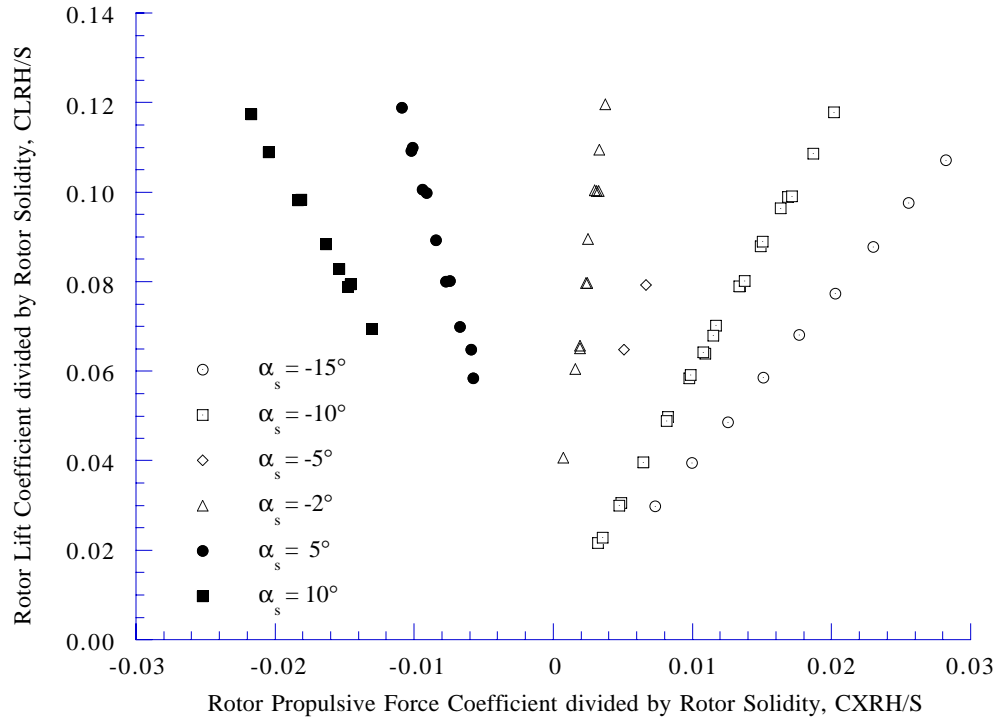


Figure 11(a). Rotor lift coefficient as a function of rotor propulsive force coefficient, 60 knots ($\mu = 0.15$).

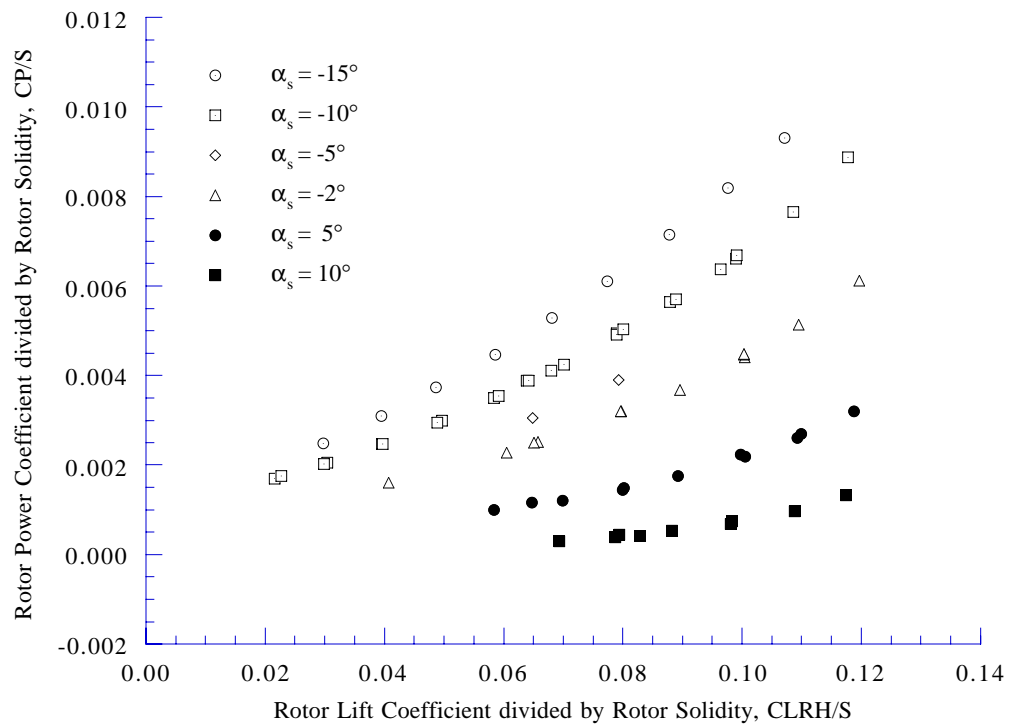


Figure 11(b). Rotor power coefficient as a function of rotor lift coefficient, 60 knots ($\mu = 0.15$).

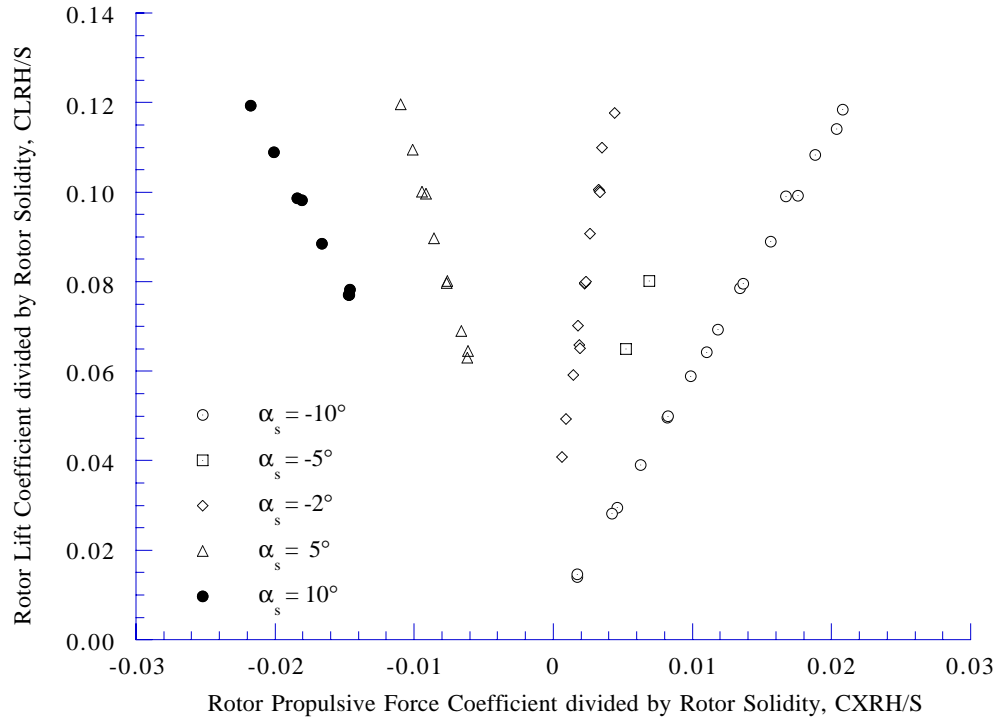


Figure 12(a). Rotor lift coefficient as a function of rotor propulsive force coefficient, 80 knots ($\mu = 0.20$).

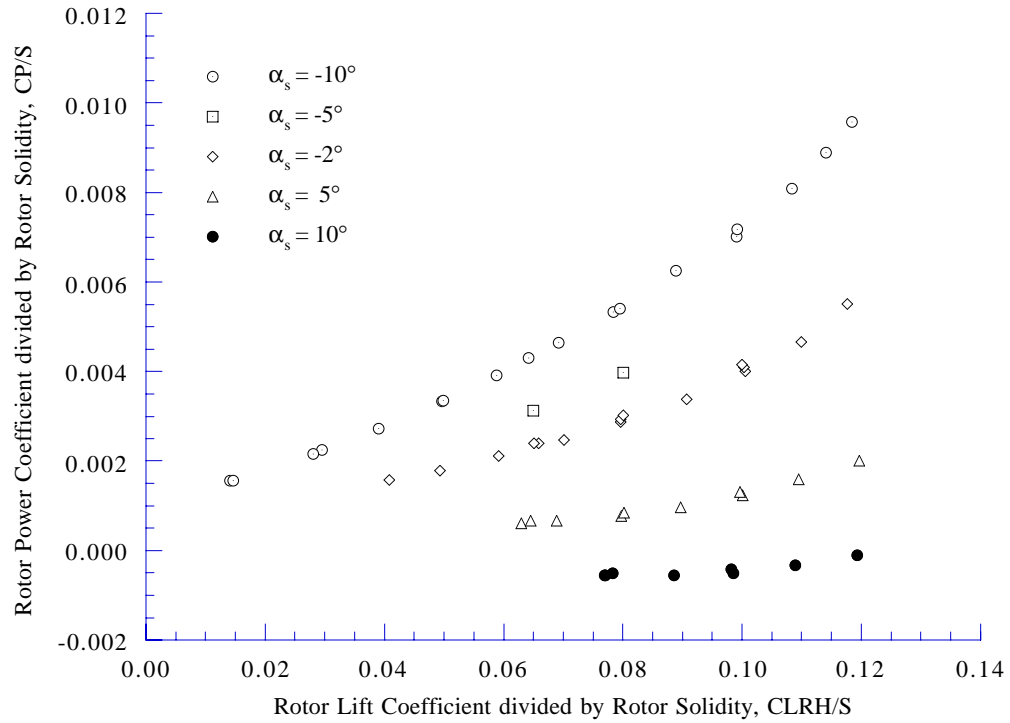


Figure 12(b). Rotor power coefficient as a function of rotor lift coefficient, 80 knots ($\mu = 0.20$).

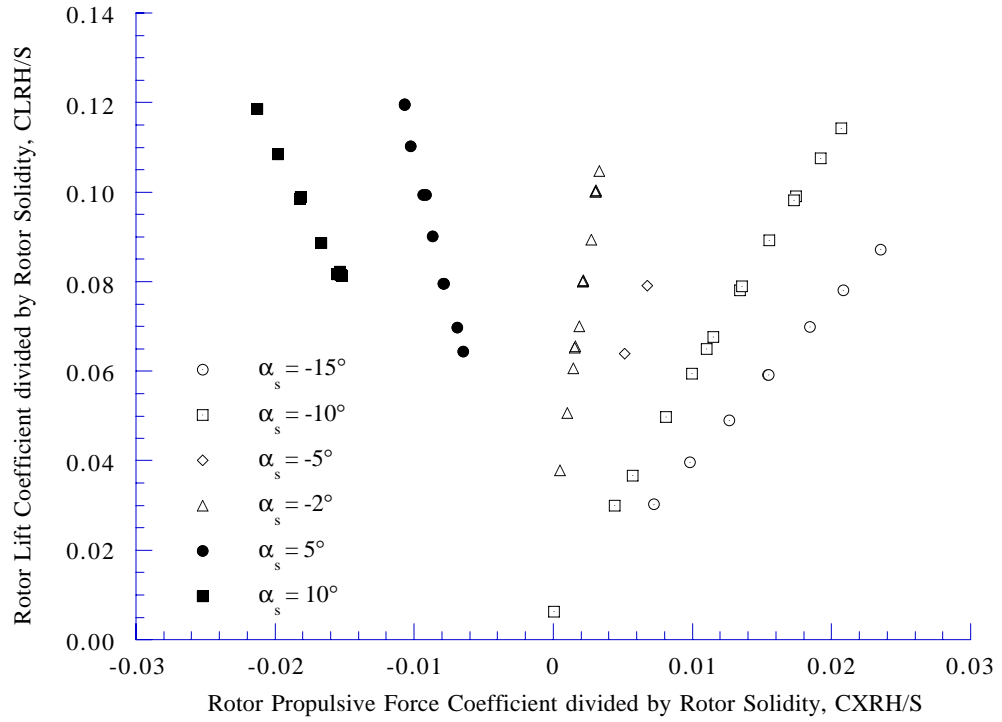


Figure 13(a). Rotor lift coefficient as a function of rotor propulsive force coefficient, 100 knots ($\mu = 0.25$).

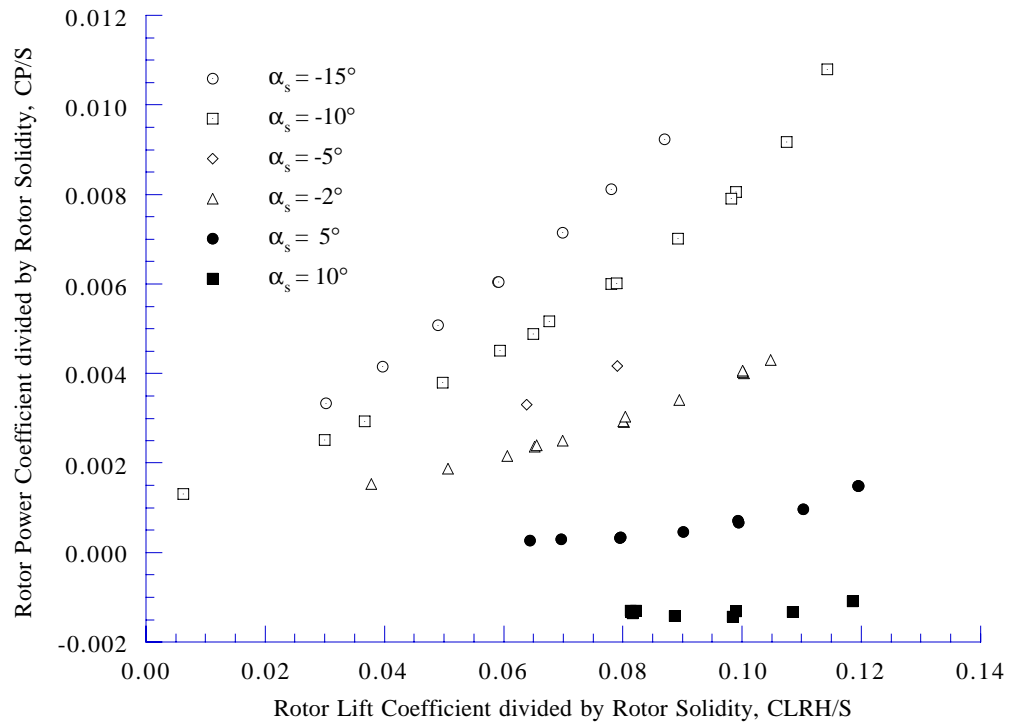


Figure 13(b). Rotor power coefficient as a function of rotor lift coefficient , 100 knots ($\mu = 0.25$).

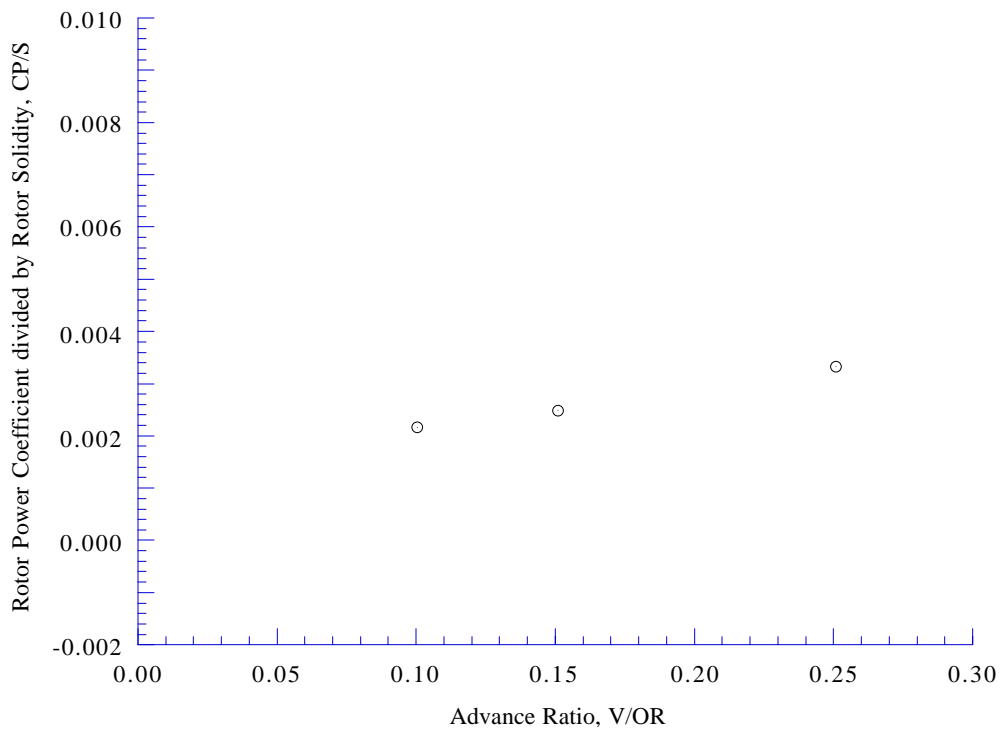


Figure 14(a). Rotor power coefficient as a function of advance ratio, $\alpha_S = -15 \text{ deg}$, $CT/\sigma = 0.030$.

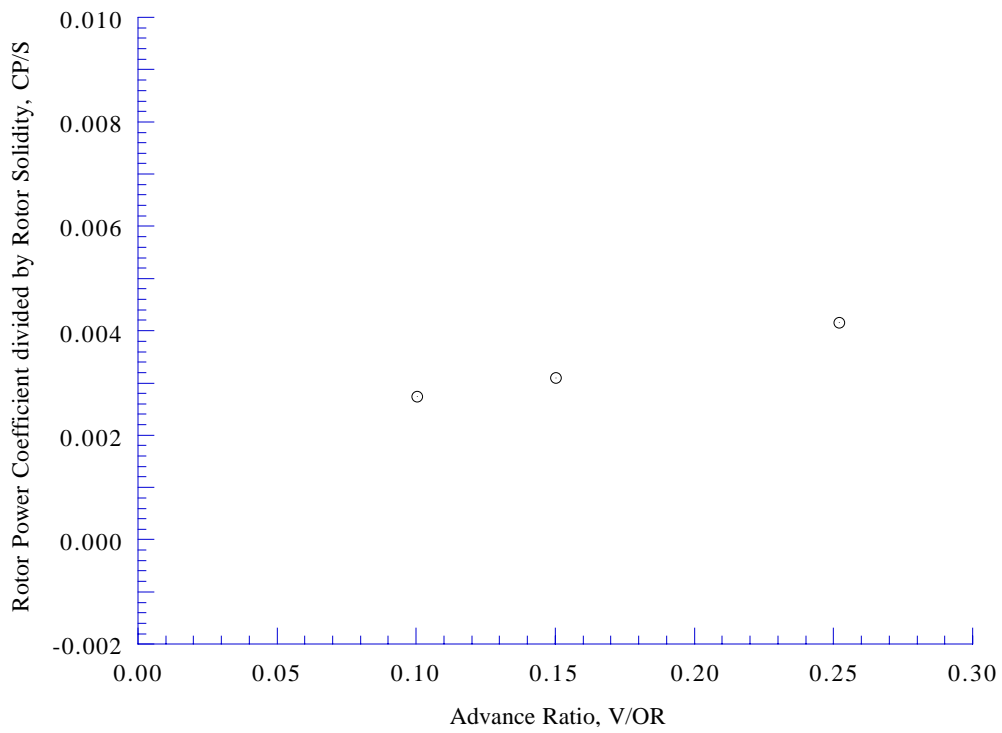


Figure 14(b). Rotor power coefficient as a function of advance ratio, $\alpha_S = -15 \text{ deg}$, $CT/\sigma = 0.040$.

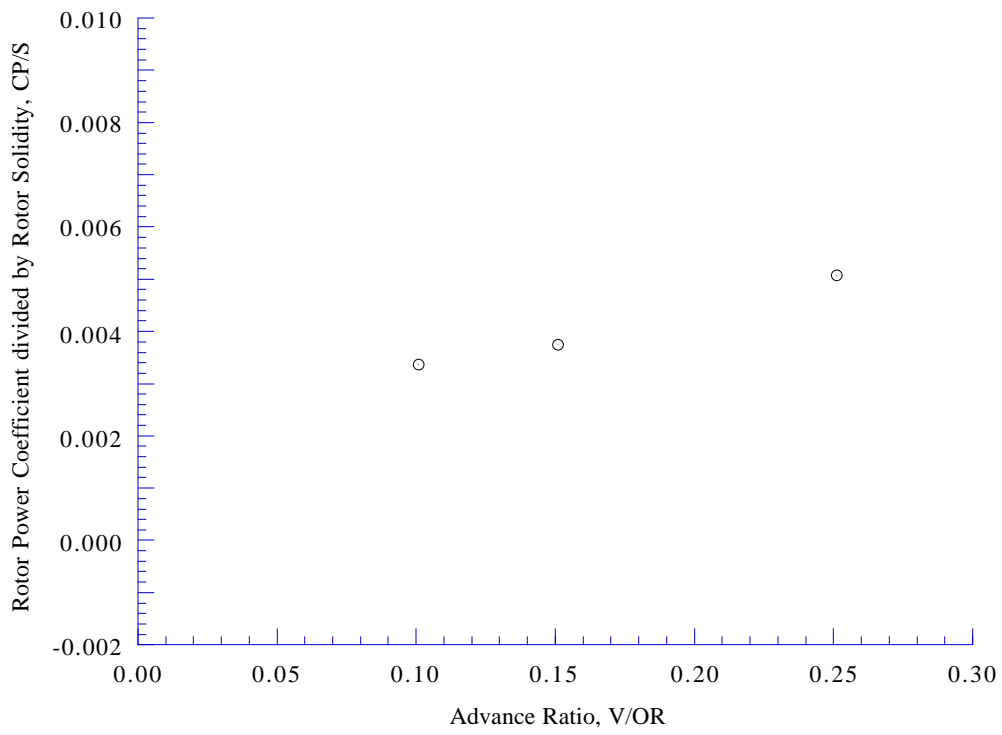


Figure 14(c). Rotor power coefficient as a function of advance ratio, $\alpha_S = -15 \text{ deg}$, $CT/\sigma = 0.050$.

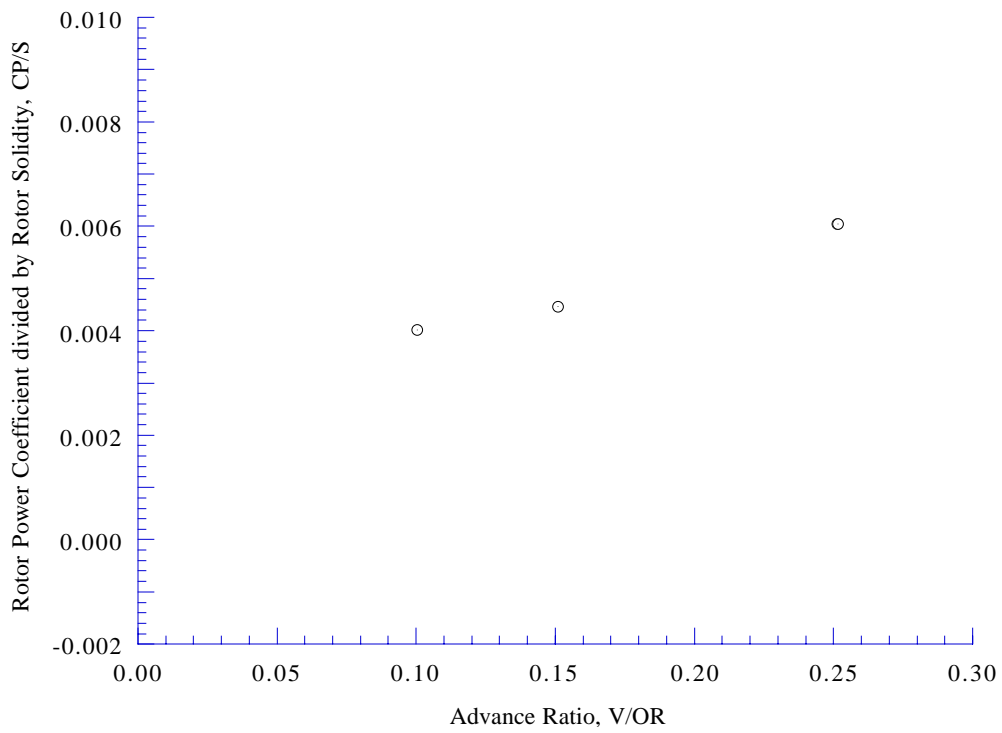


Figure 14(d). Rotor power coefficient as a function of advance ratio, $\alpha_S = -15 \text{ deg}$, $CT/\sigma = 0.060$.

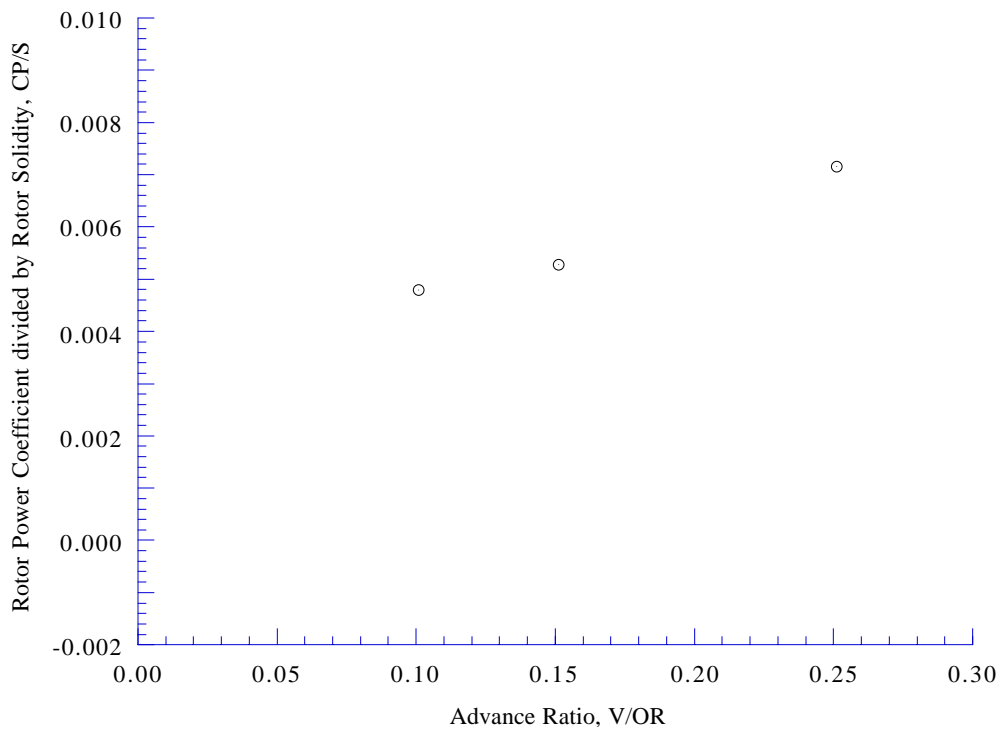


Figure 14(e). Rotor power coefficient as a function of advance ratio, $\alpha_S = -15 \text{ deg}$, $C_T/\sigma = 0.070$.

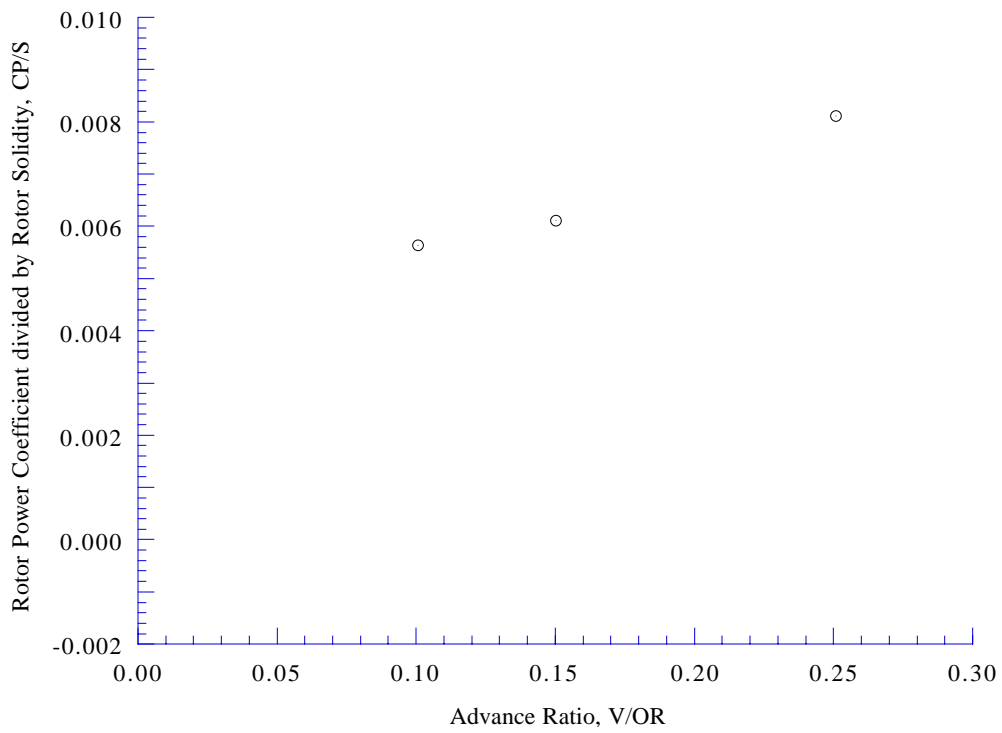


Figure 14(f). Rotor power coefficient as a function of advance ratio, $\alpha_S = -15 \text{ deg}$, $C_T/\sigma = 0.080$.

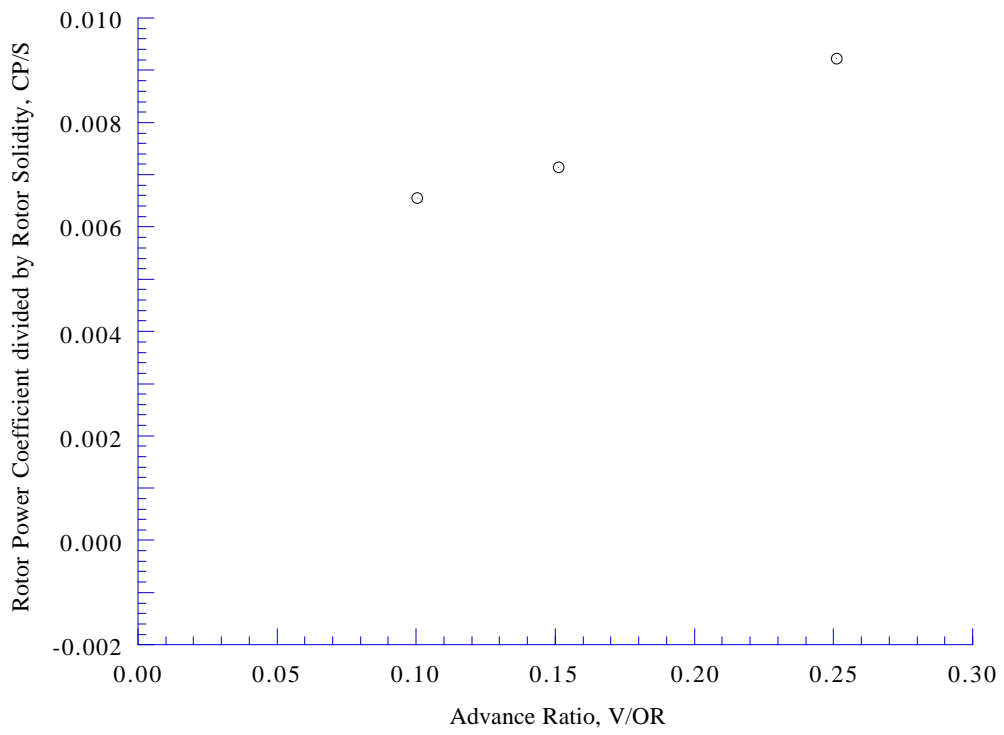


Figure 14(g). Rotor power coefficient as a function of advance ratio, $\alpha_S = -15 \text{ deg}$, $C_T/\sigma = 0.090$.

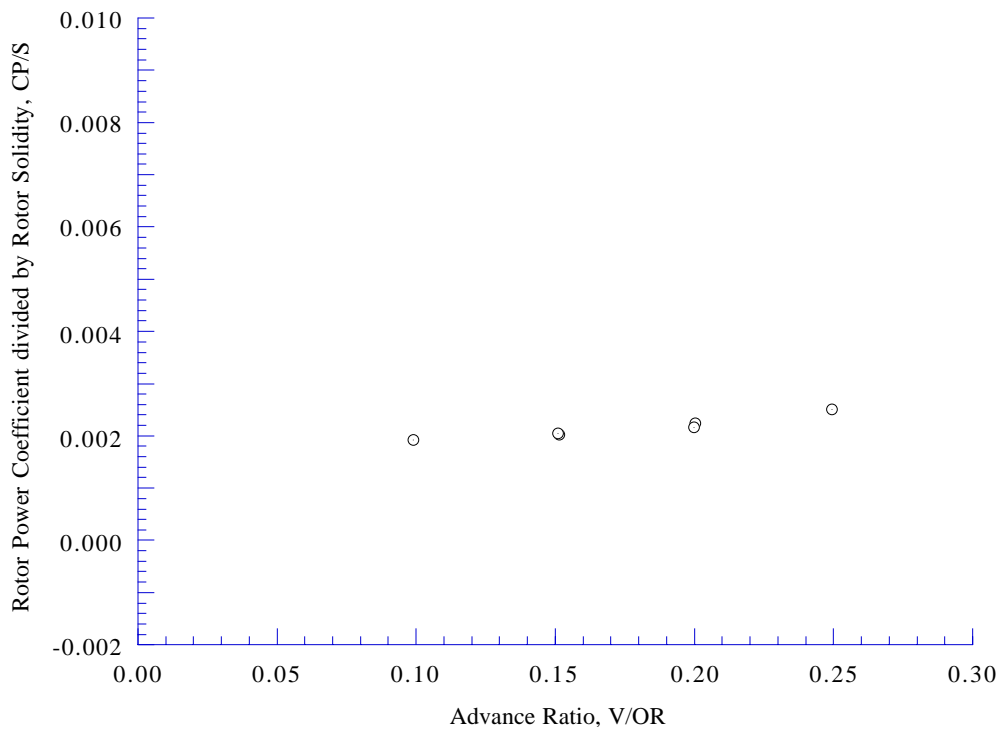


Figure 15(a). Rotor power coefficient as a function of advance ratio, $\alpha_S = -10 \text{ deg}$, $C_T/\sigma = 0.030$.

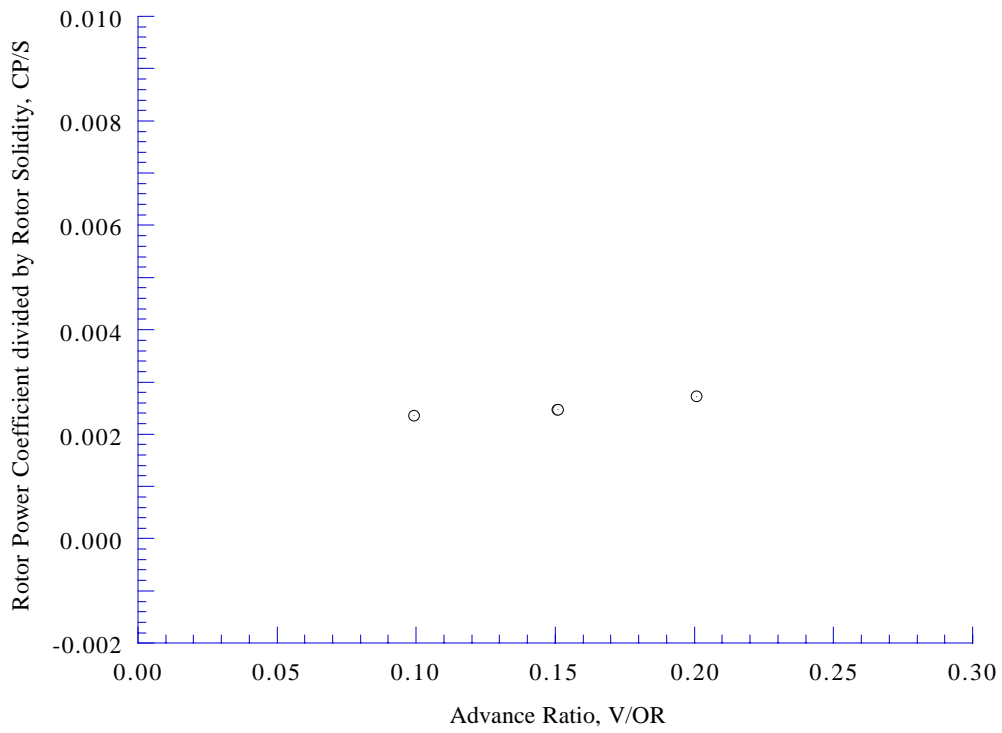


Figure 15(b). Rotor power coefficient as a function of advance ratio, $\alpha_S = -10 \text{ deg}$, $C_T/\sigma = 0.040$.

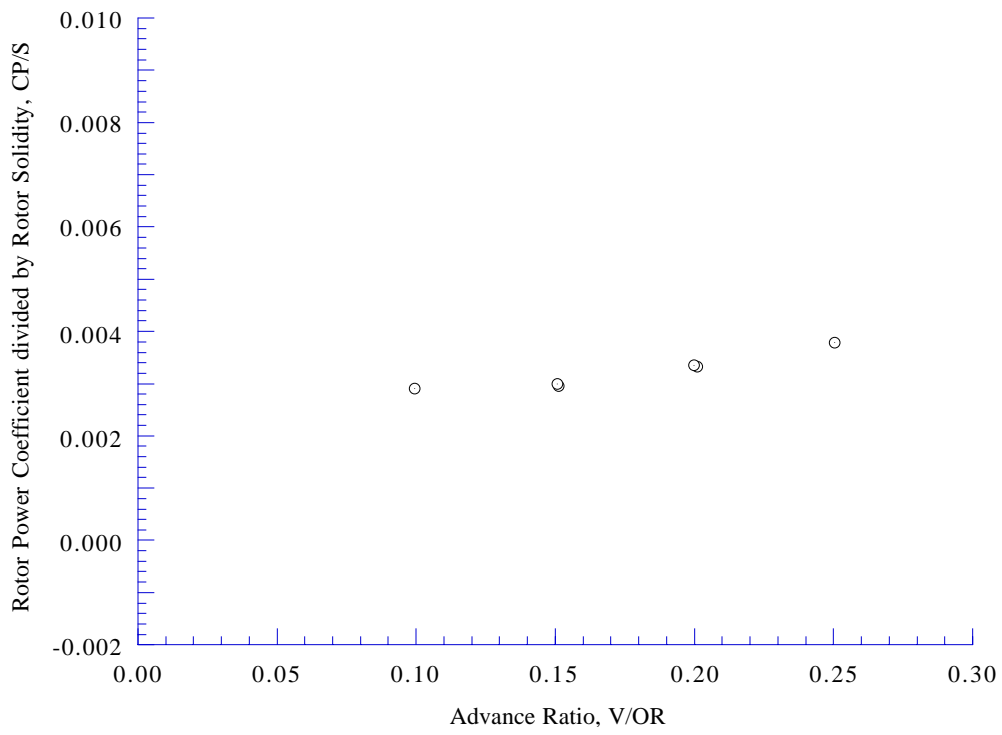


Figure 15(c). Rotor power coefficient as a function of advance ratio, $\alpha_S = -10 \text{ deg}$, $C_T/\sigma = 0.050$.

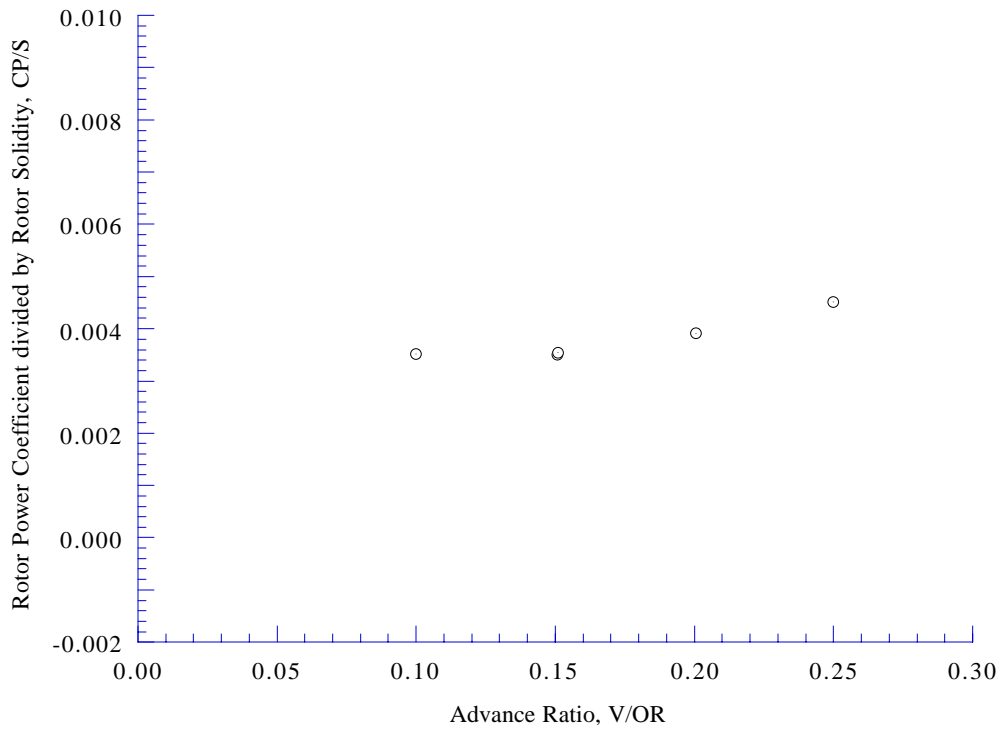


Figure 15(d). Rotor power coefficient as a function of advance ratio, $\alpha_S = -10 \text{ deg}$, $C_T/\sigma = 0.060$.

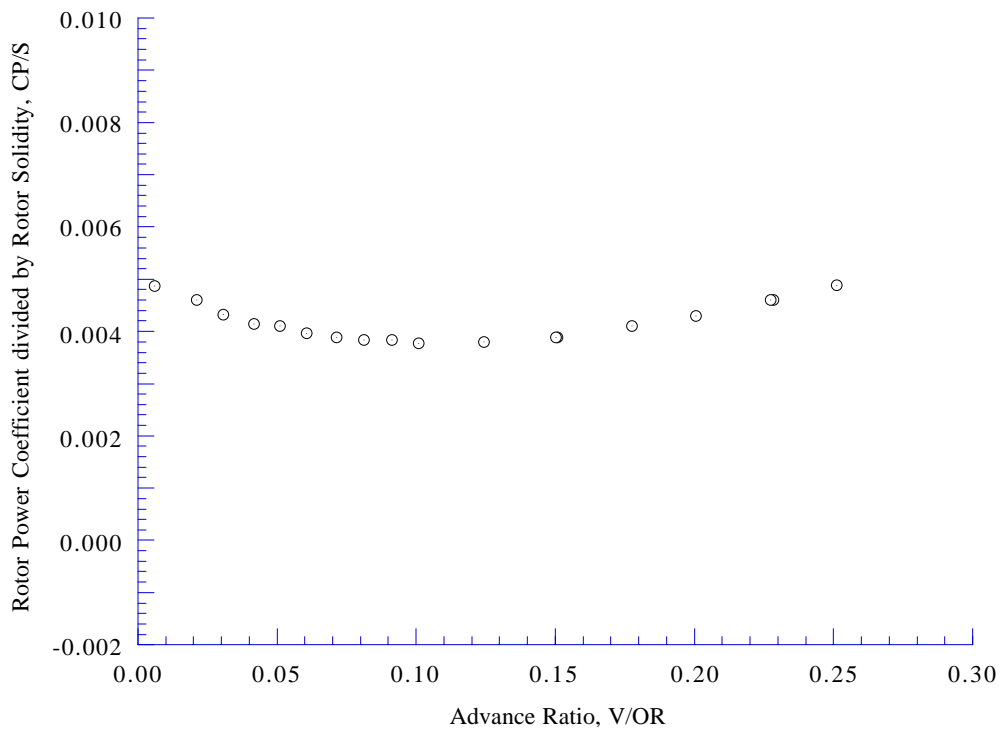


Figure 15(e). Rotor power coefficient as a function of advance ratio, $\alpha_S = -10 \text{ deg}$, $C_T/\sigma = 0.065$.

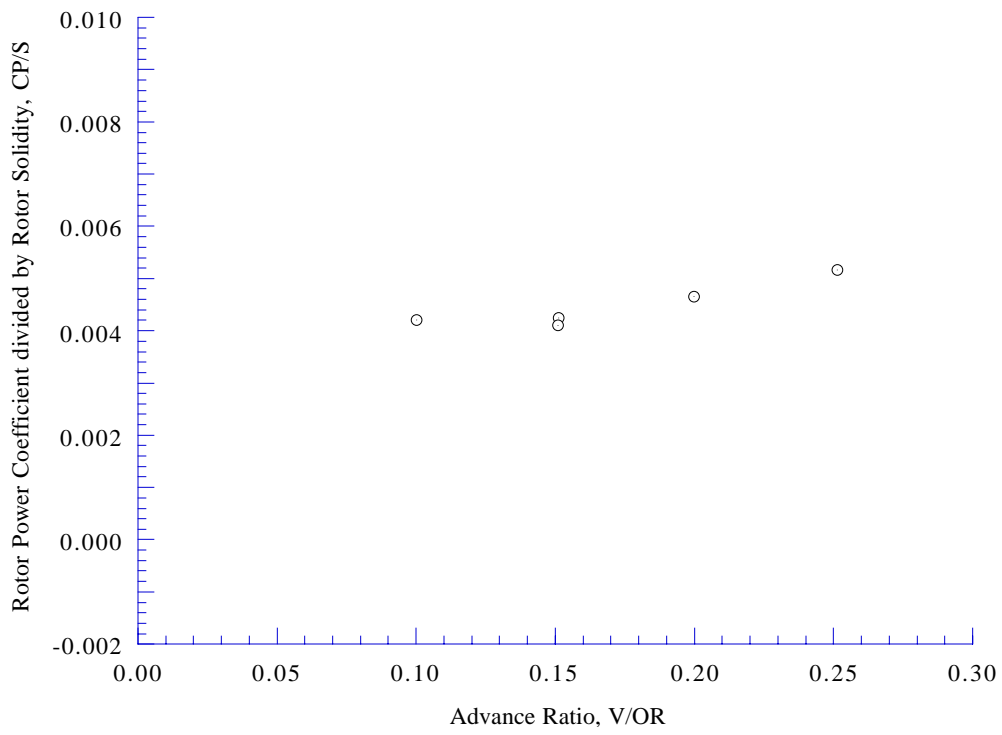


Figure 15(f). Rotor power coefficient as a function of advance ratio, $\alpha_S = -10 \text{ deg}$, $C_T/\sigma = 0.070$.

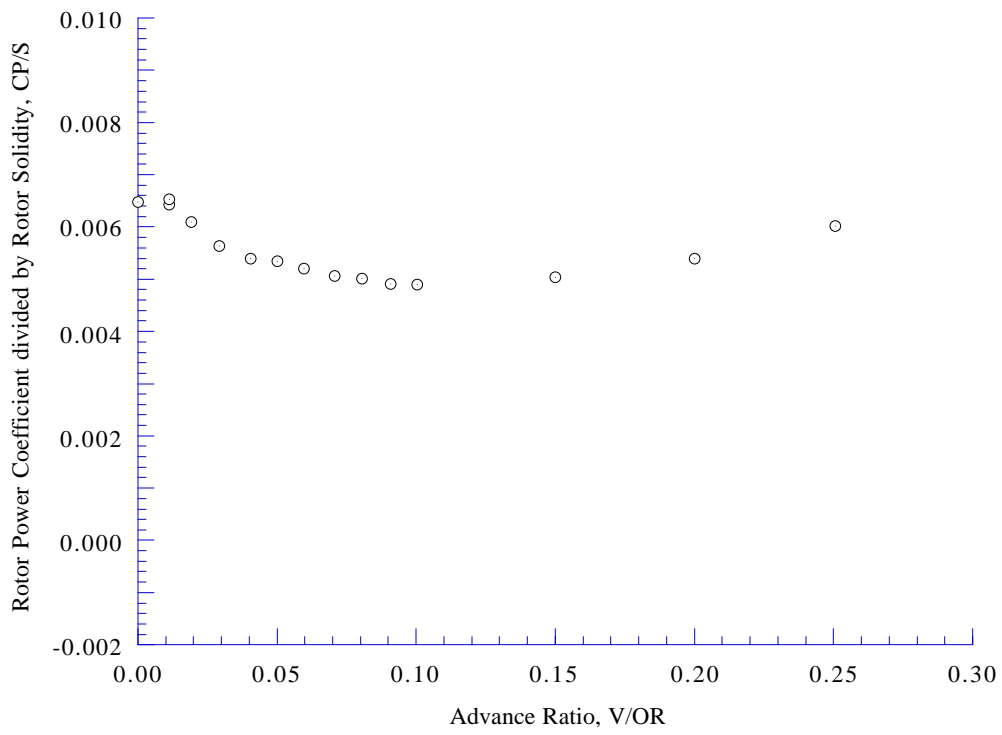


Figure 15(g). Rotor power coefficient as a function of advance ratio, $\alpha_S = -10 \text{ deg}$, $C_T/\sigma = 0.080$.

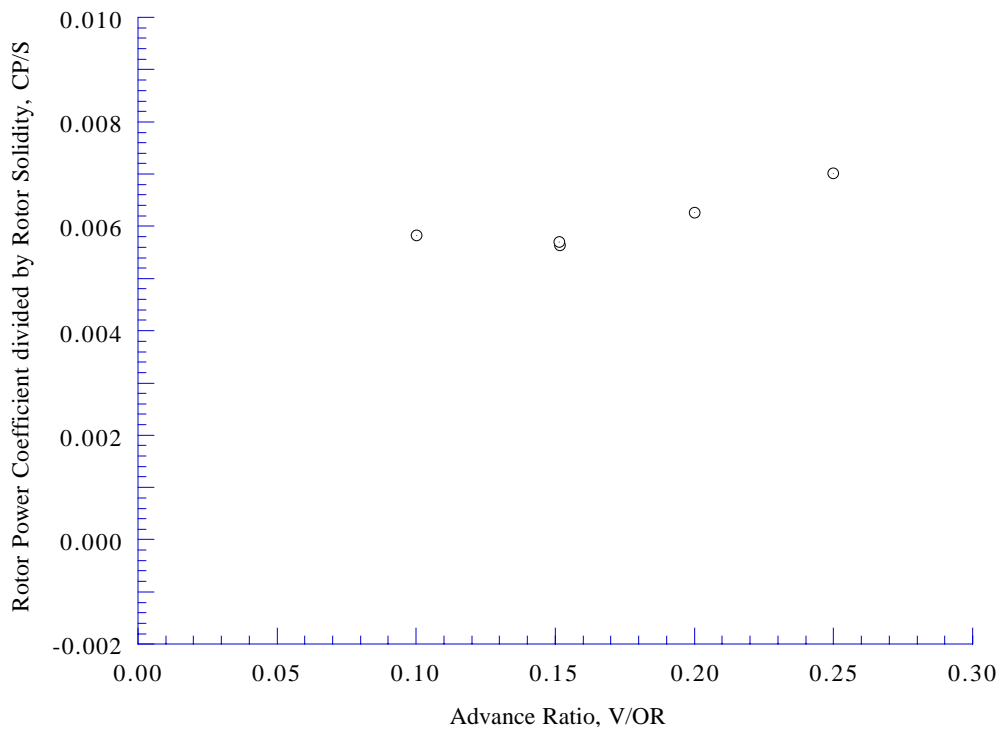


Figure 15(h). Rotor power coefficient as a function of advance ratio, $\alpha_S = -10 \text{ deg}$, $C_T/\sigma = 0.090$.

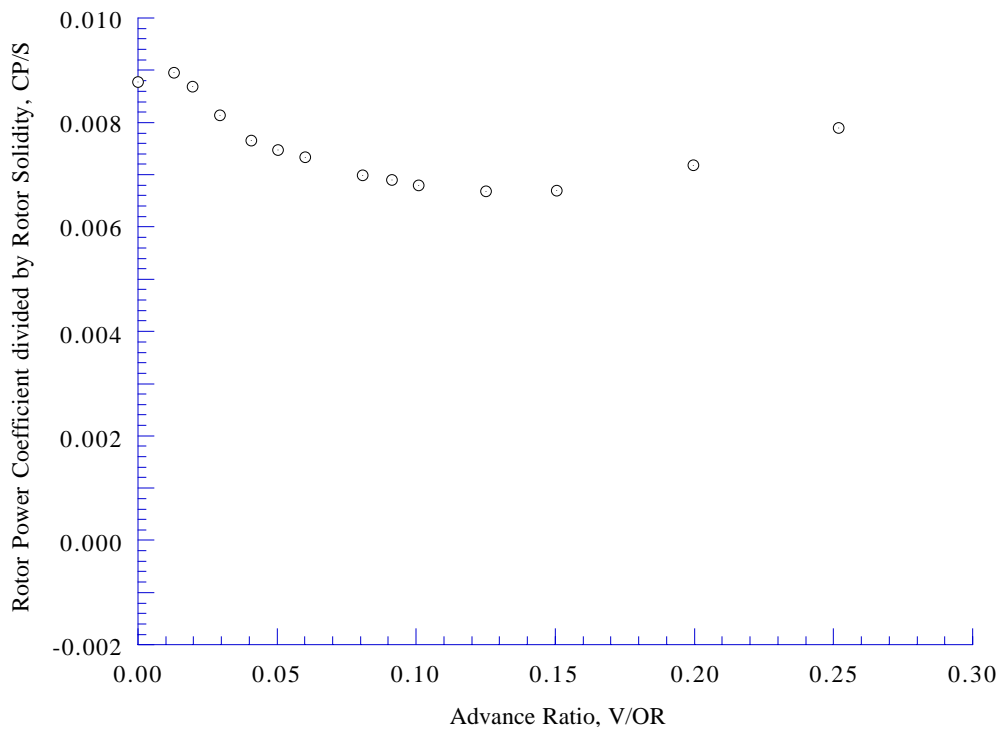


Figure 15(i). Rotor power coefficient as a function of advance ratio, $\alpha_S = -10 \text{ deg}$, $C_T/\sigma = 0.100$.

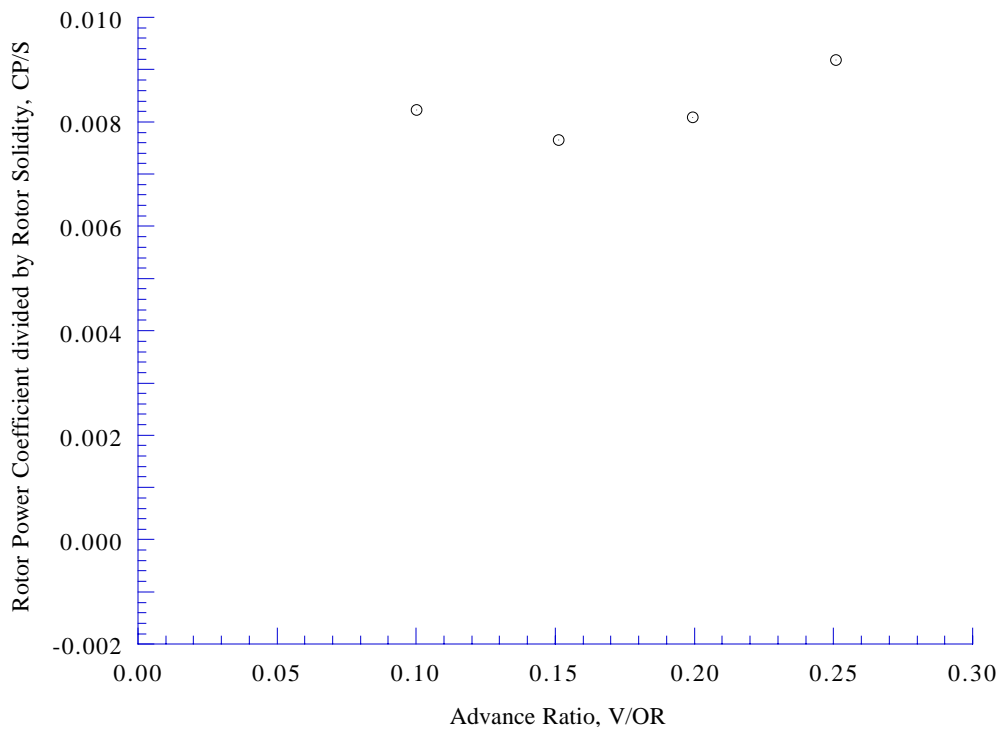


Figure 15(j). Rotor power coefficient as a function of advance ratio, $\alpha_S = -10 \text{ deg}$, $C_T/\sigma = 0.110$.

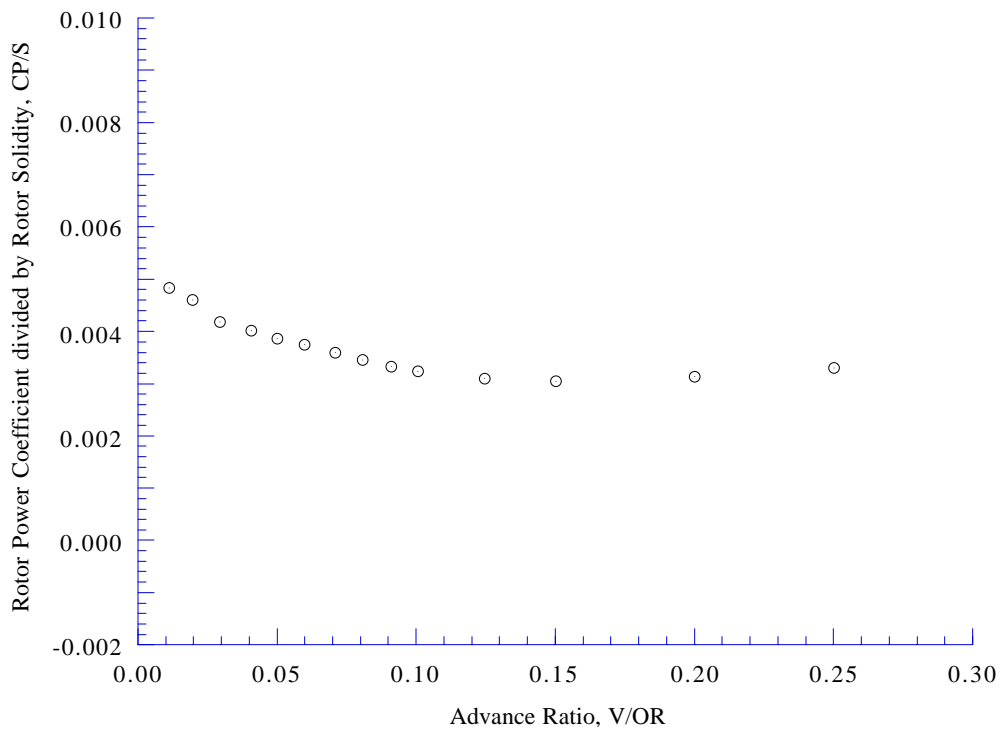


Figure 16(a). Rotor power coefficient as a function of advance ratio, $\alpha_S = -5 \text{ deg}$, $C_T/\sigma = 0.065$.

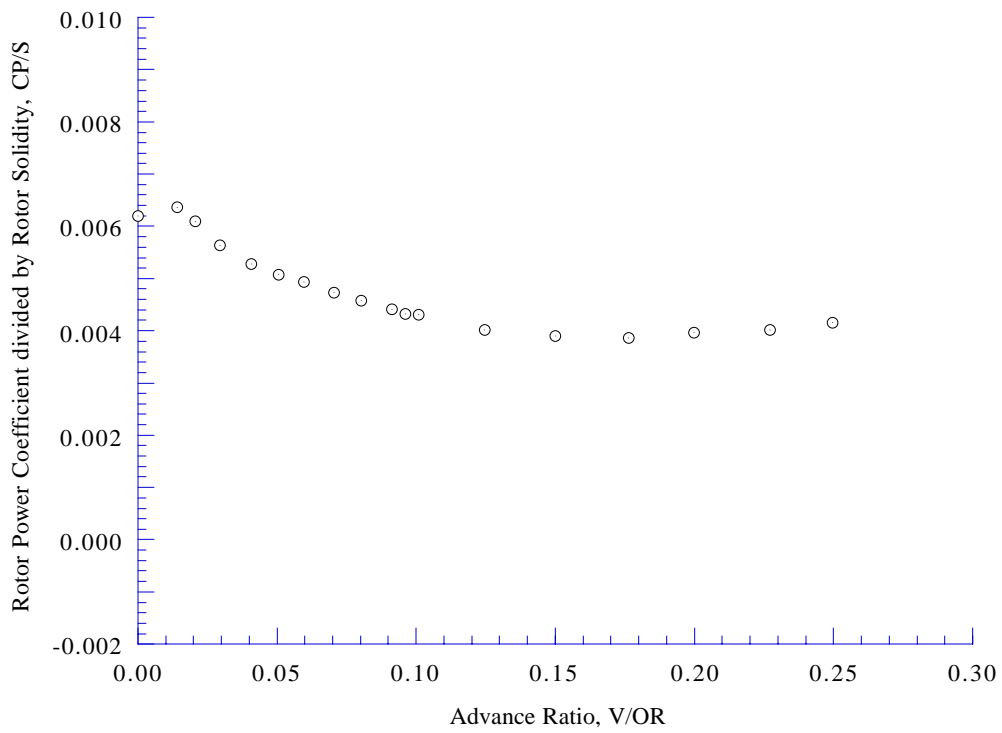


Figure 16(b). Rotor power coefficient as a function of advance ratio, $\alpha_S = -5 \text{ deg}$, $C_T/\sigma = 0.080$.

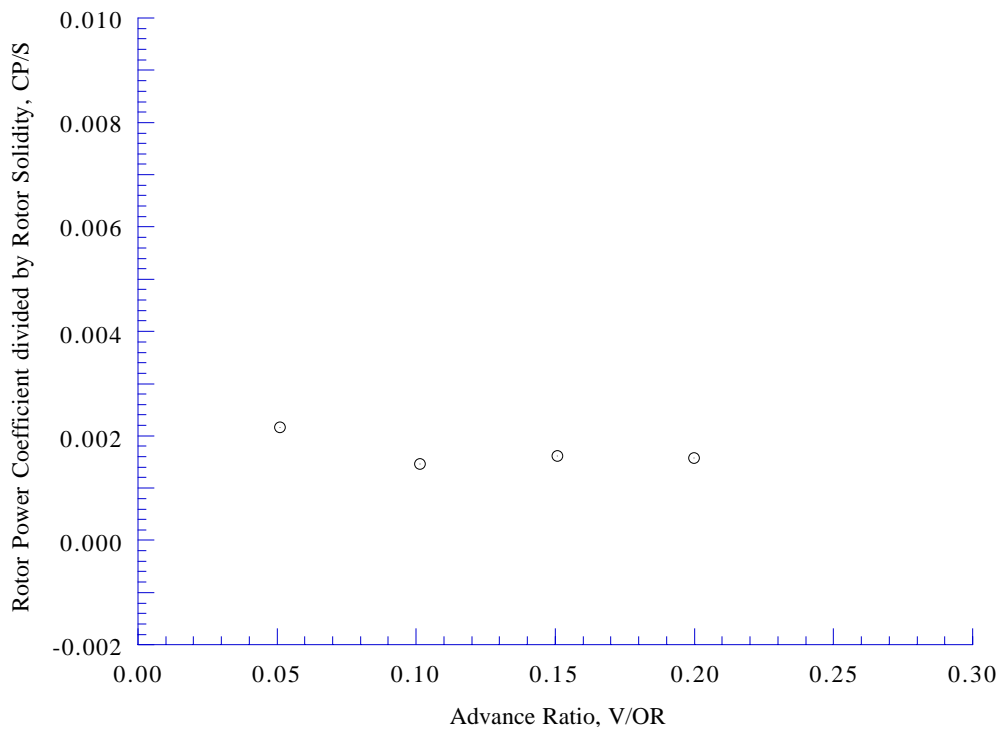


Figure 17(a). Rotor power coefficient as a function of advance ratio, $\alpha_S = -2$ deg, $C_T/\sigma = 0.040$.

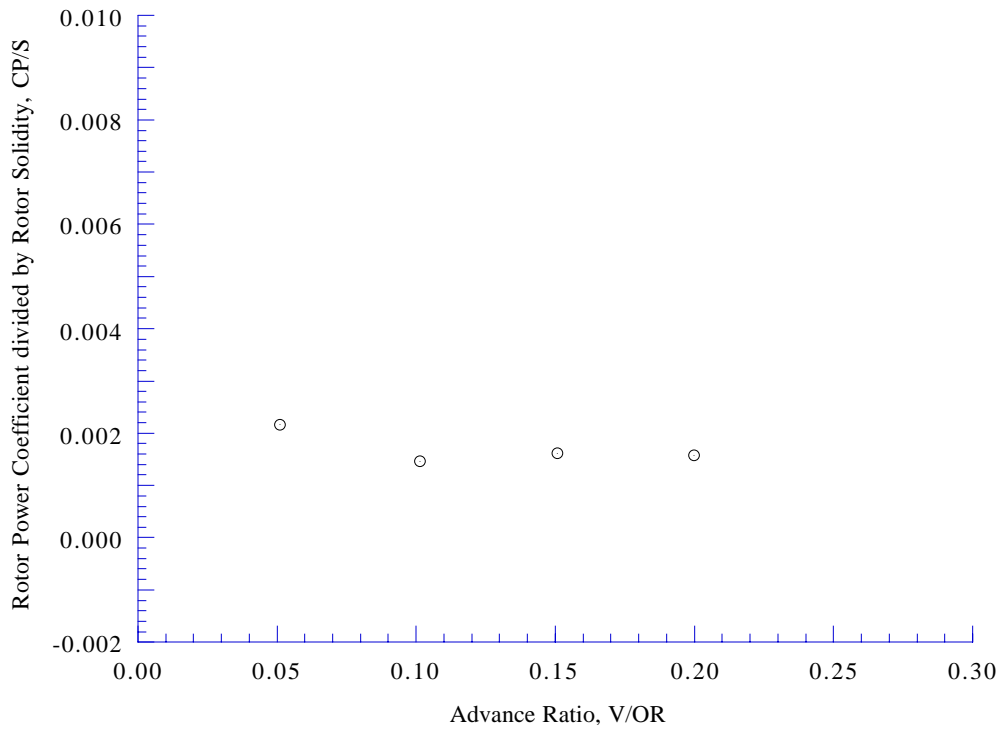


Figure 17(b). Rotor power coefficient as a function of advance ratio, $\alpha_S = -2$ deg, $C_T/\sigma = 0.050$.

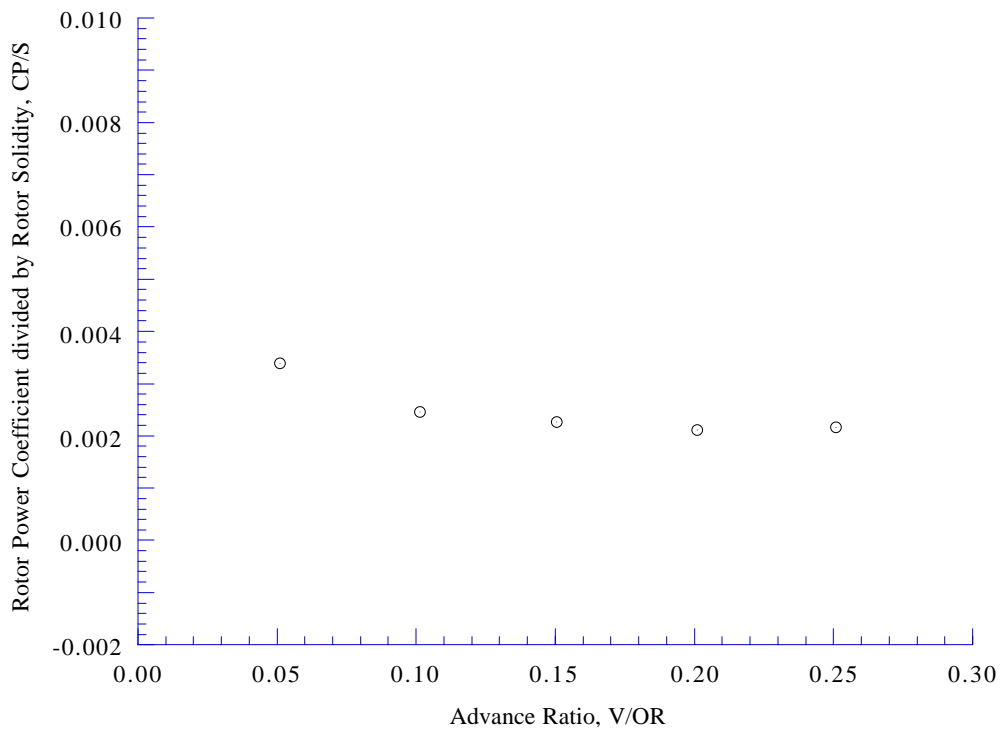


Figure 17(c). Rotor power coefficient as a function of advance ratio, $\alpha_S = -2$ deg, $C_T/\sigma = 0.060$.

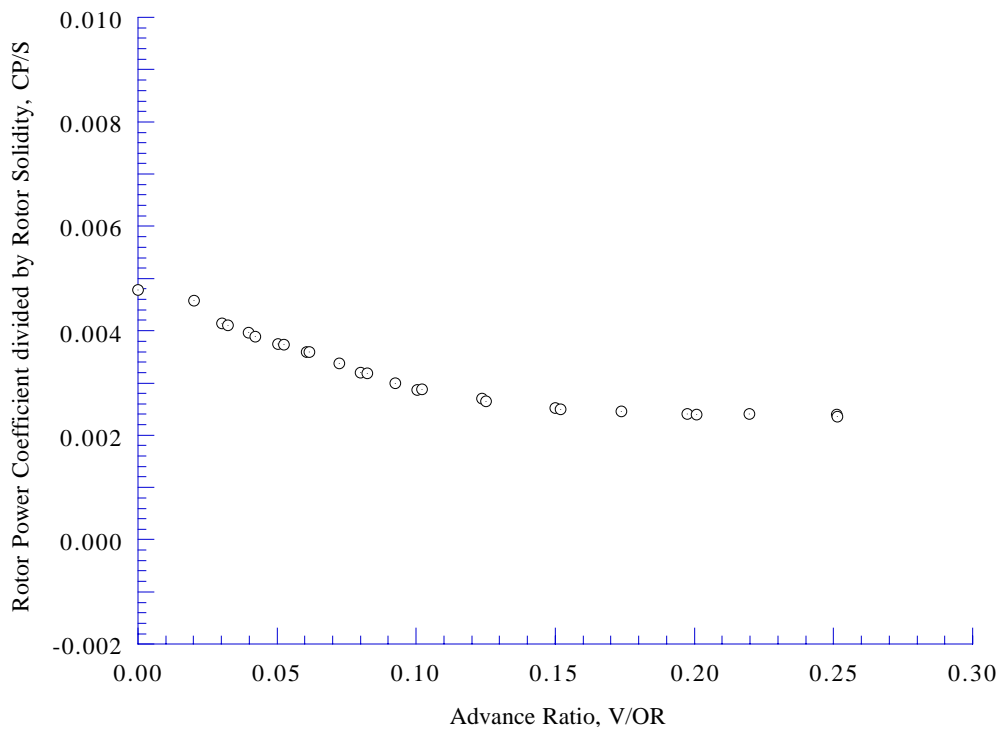


Figure 17(d). Rotor power coefficient as a function of advance ratio, $\alpha_S = -2$ deg, $C_T/\sigma = 0.065$.

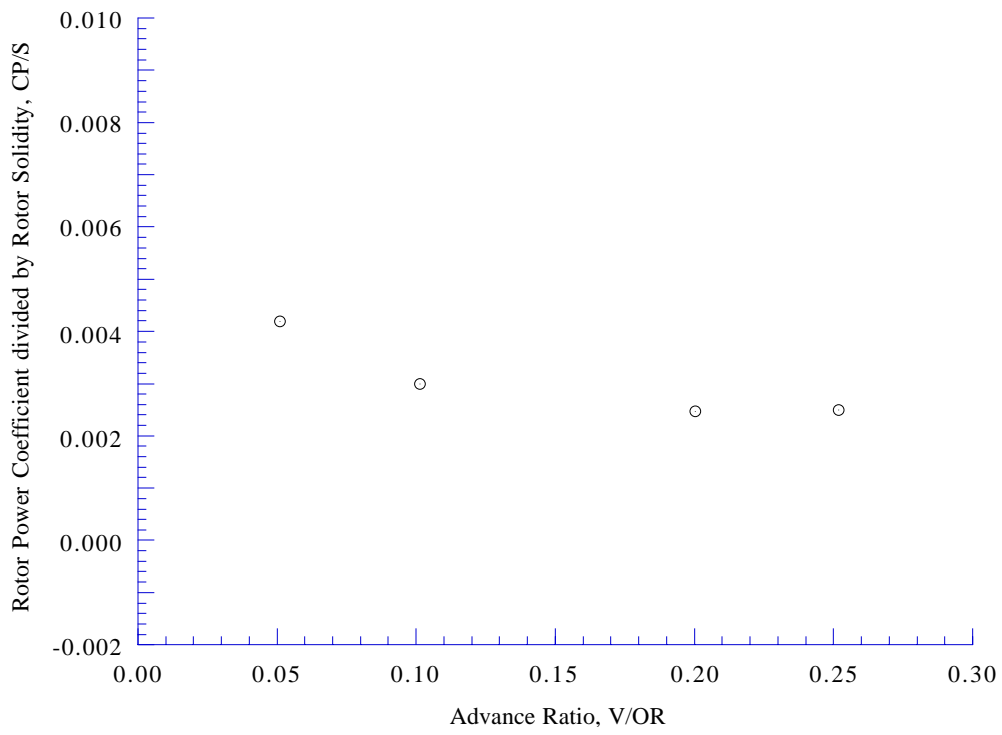


Figure 17(e). Rotor power coefficient as a function of advance ratio, $\alpha_S = -2 \text{ deg}$, $C_T/\sigma = 0.070$.

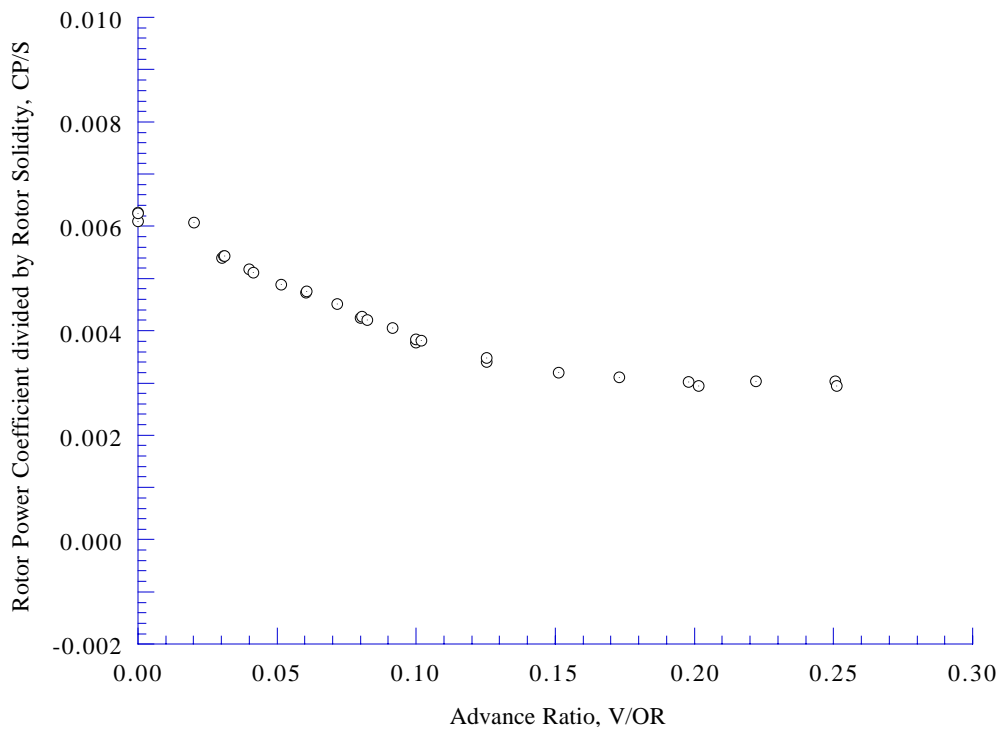


Figure 17(f). Rotor power coefficient as a function of advance ratio, $\alpha_S = -2 \text{ deg}$, $C_T/\sigma = 0.080$.

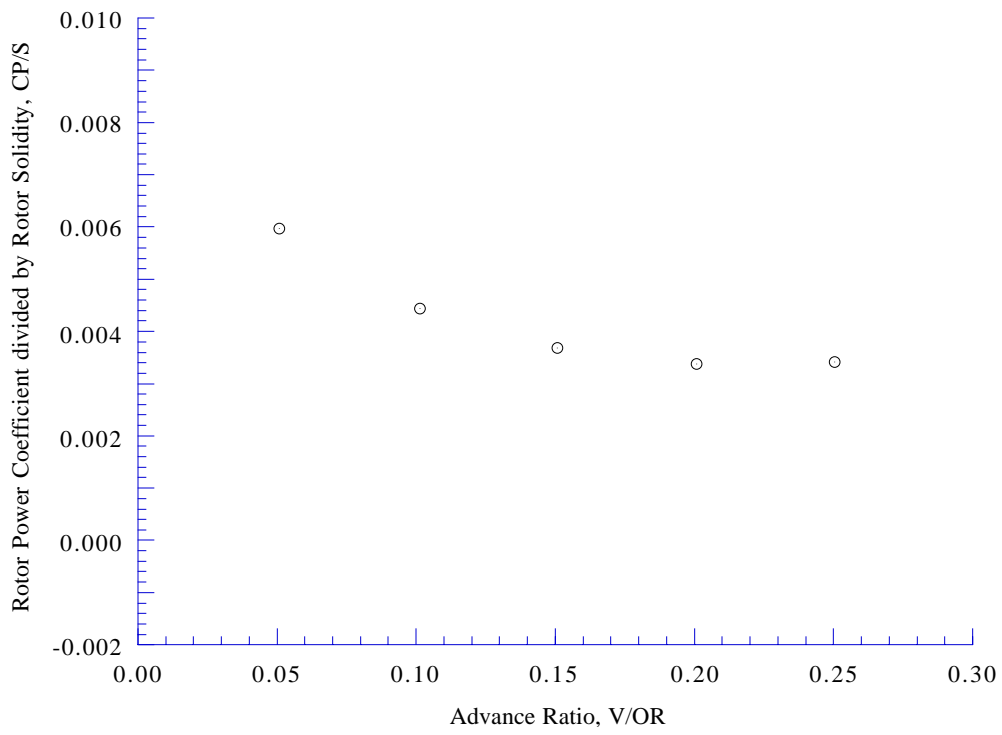


Figure 17(g). Rotor power coefficient as a function of advance ratio, $\alpha_S = -2$ deg, $C_T/\sigma = 0.090$.

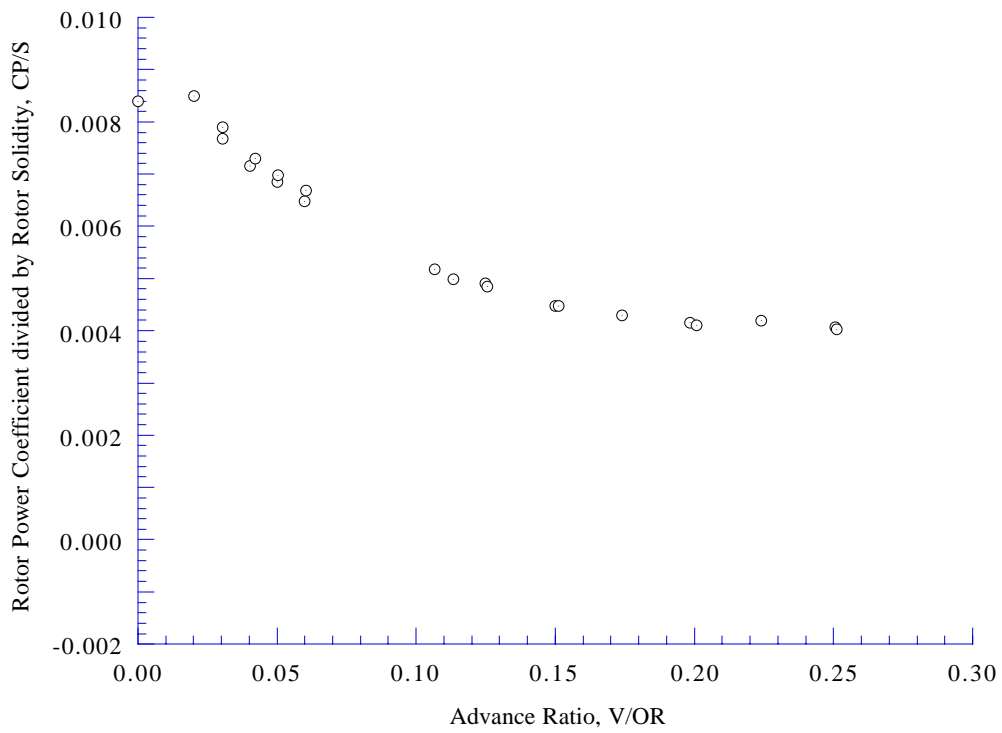


Figure 17(h). Rotor power coefficient as a function of advance ratio, $\alpha_S = -2$ deg, $C_T/\sigma = 0.100$.

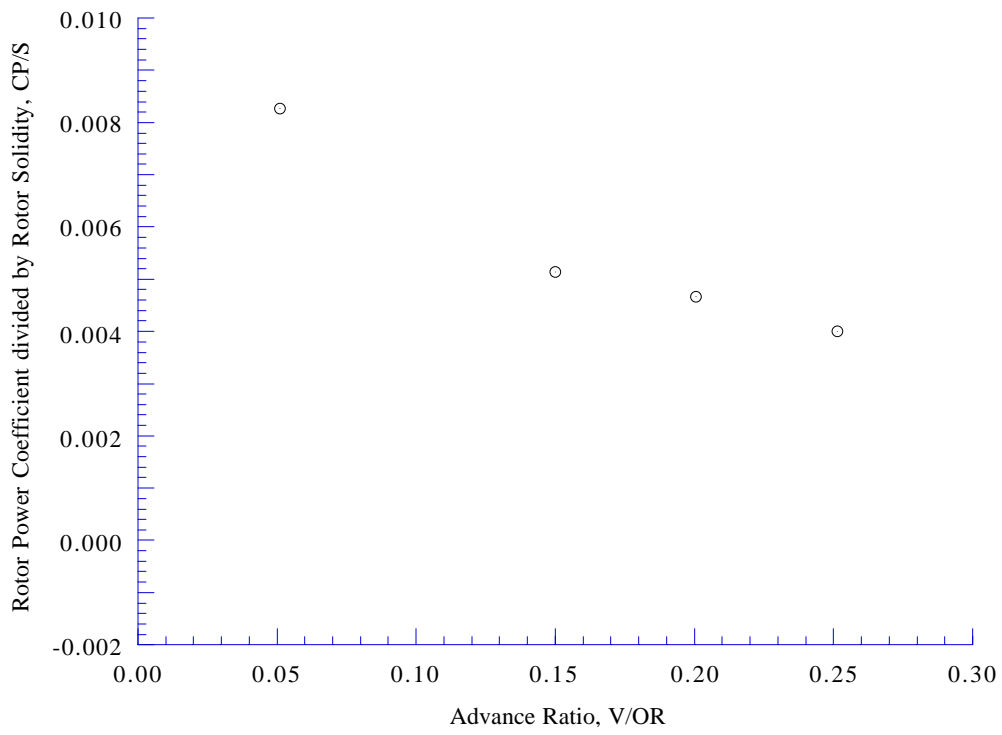


Figure 17(i). Rotor power coefficient as a function of advance ratio, $\alpha_S = -2 \text{ deg}$, $C_T/\sigma = 0.110$.

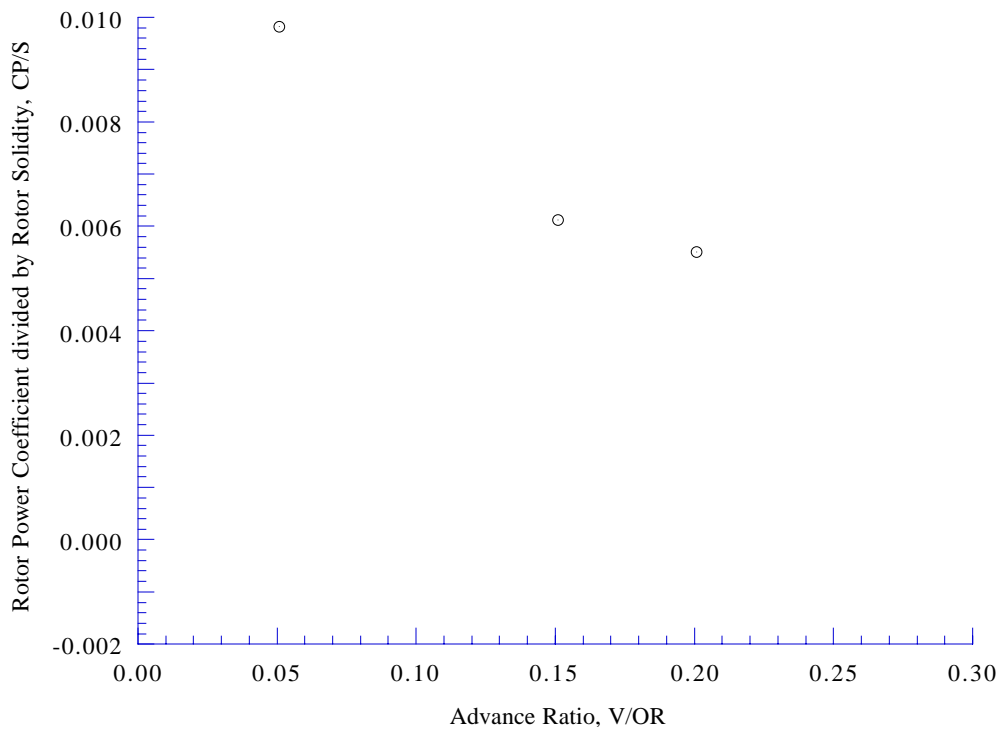


Figure 17(j). Rotor power coefficient as a function of advance ratio, $\alpha_S = -2 \text{ deg}$, $C_T/\sigma = 0.120$.

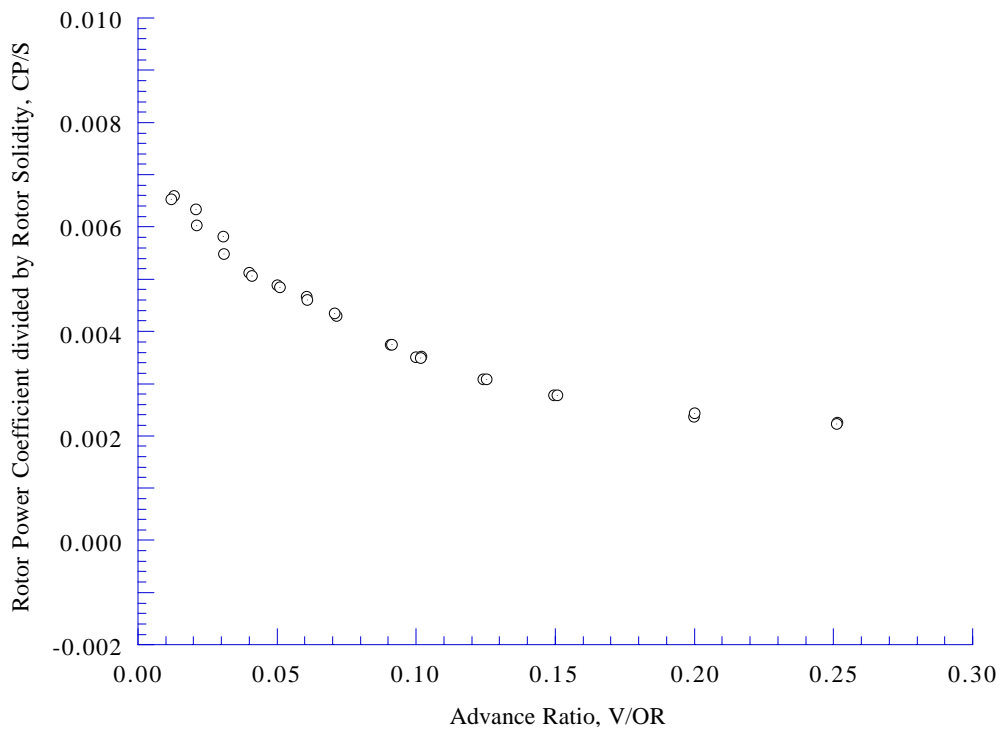


Figure 18(a). Rotor power coefficient as a function of advance ratio, $\alpha_S = 0 \text{ deg}$, $CT/\sigma = 0.080$.

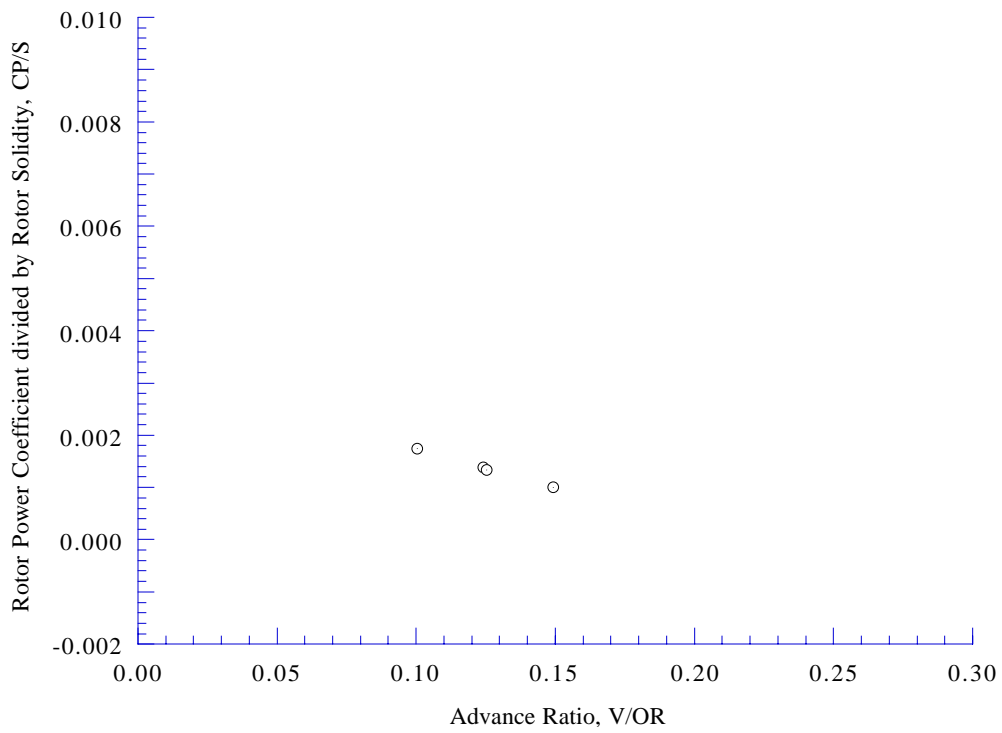


Figure 19(a). Rotor power coefficient as a function of advance ratio, $\alpha_S = 5 \text{ deg}$, $CT/\sigma = 0.060$.

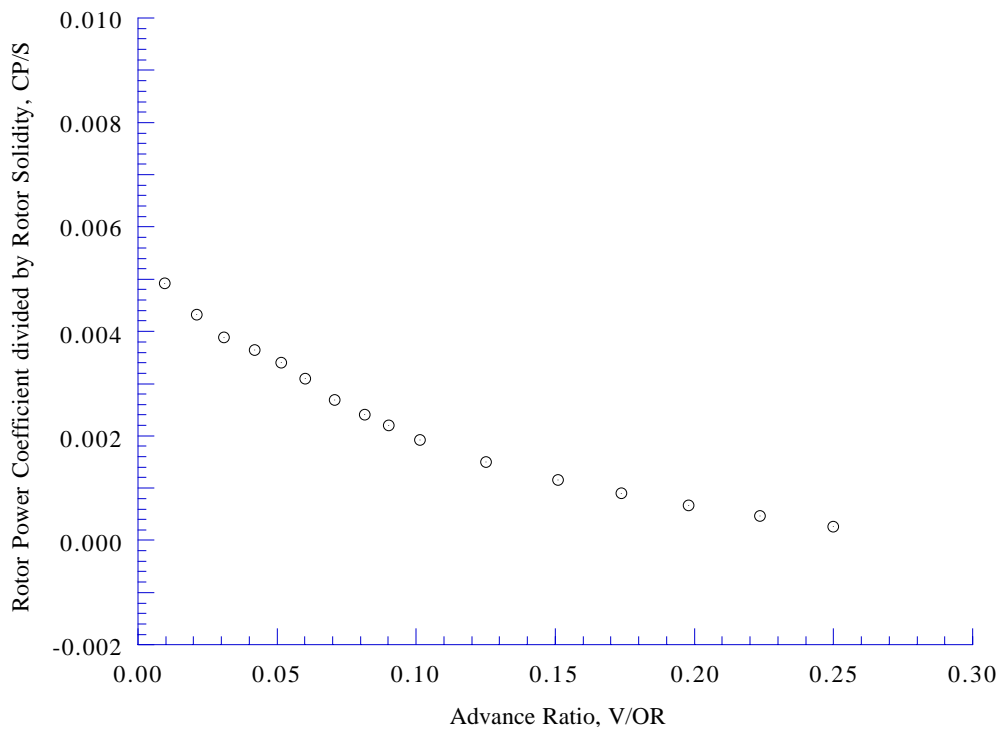


Figure 19(b). Rotor power coefficient as a function of advance ratio, $\alpha_S = 5 \text{ deg}$, $C_T/\sigma = 0.065$.

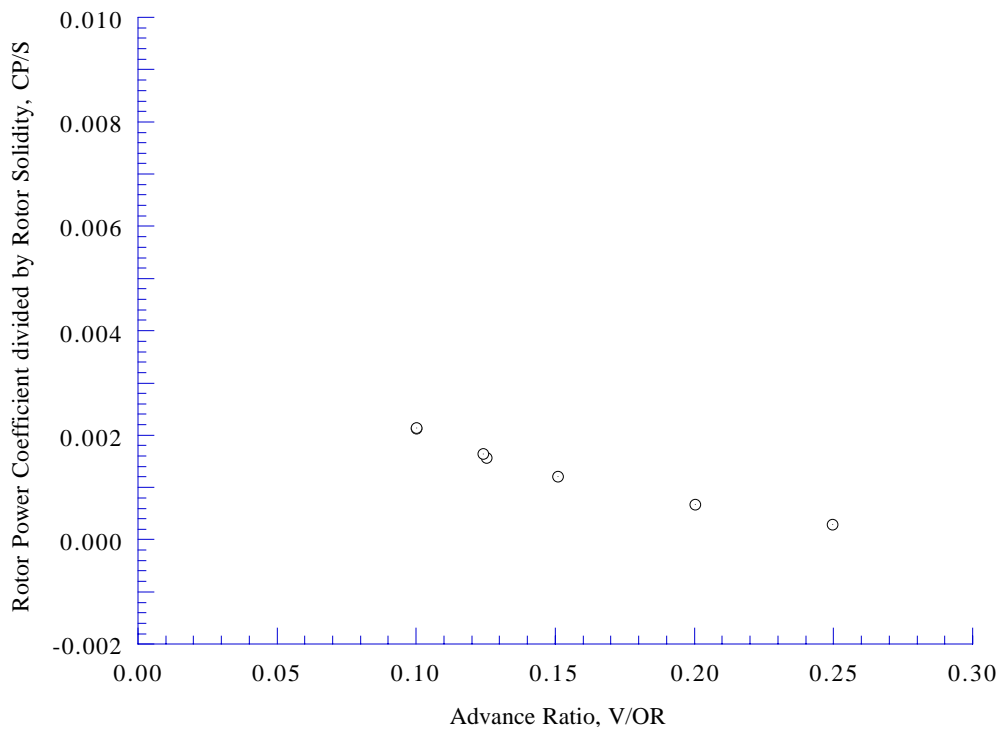


Figure 19(c). Rotor power coefficient as a function of advance ratio, $\alpha_S = 5 \text{ deg}$, $C_T/\sigma = 0.070$.

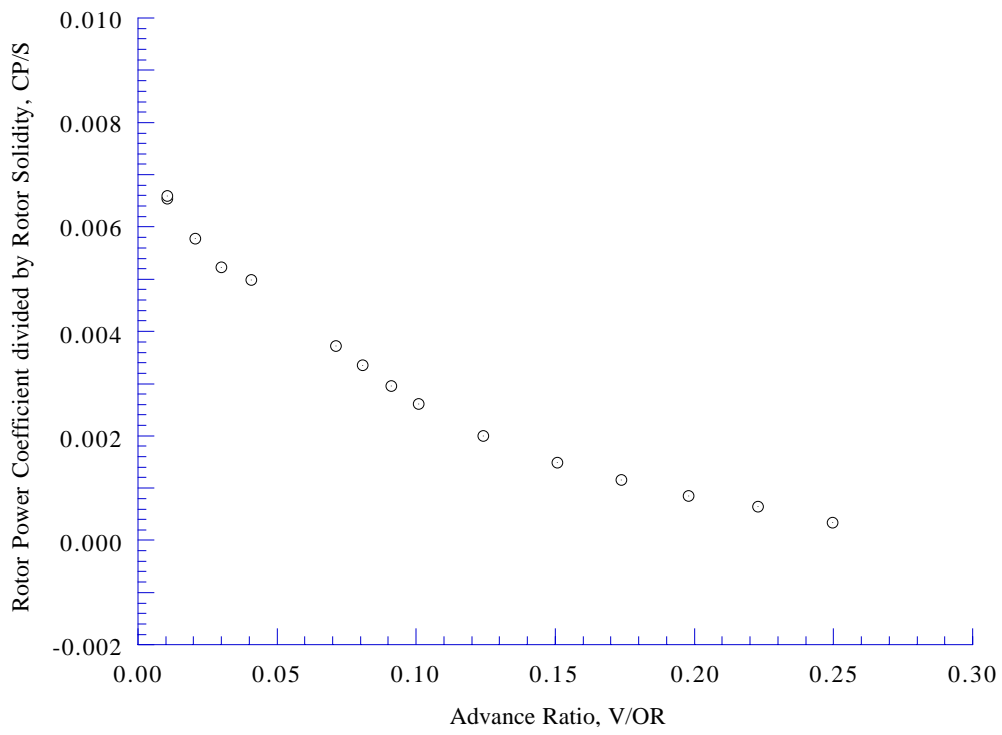


Figure 19(d). Rotor power coefficient as a function of advance ratio, $\alpha_S = 5 \text{ deg}$, $C_T/\sigma = 0.080$.

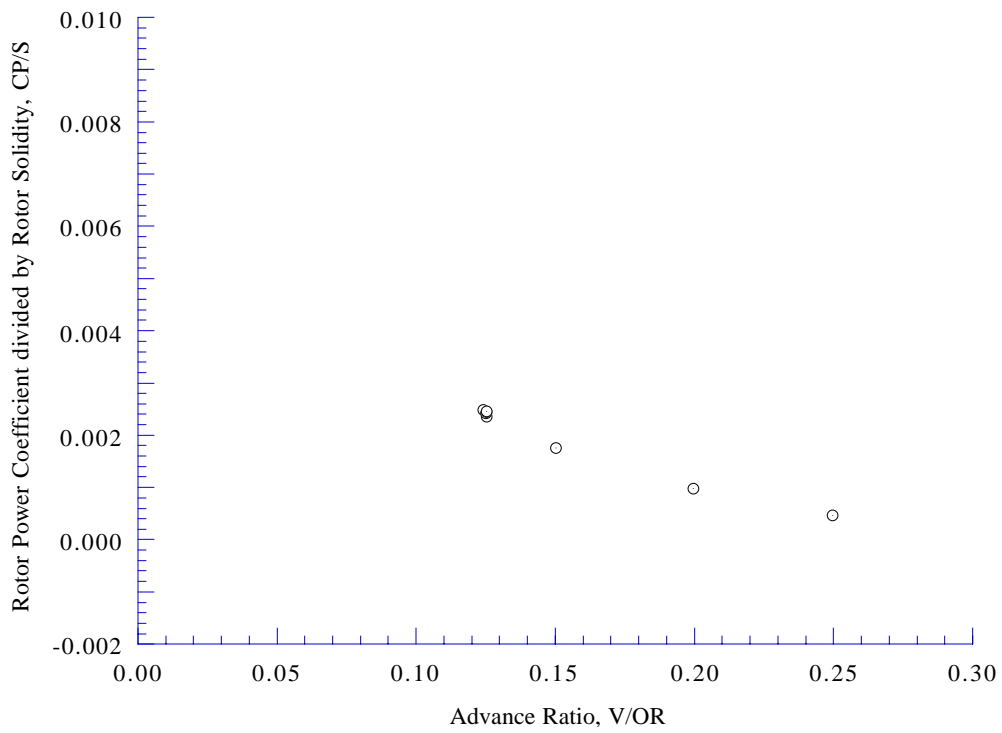


Figure 19(e). Rotor power coefficient as a function of advance ratio, $\alpha_S = 5 \text{ deg}$, $C_T/\sigma = 0.090$.

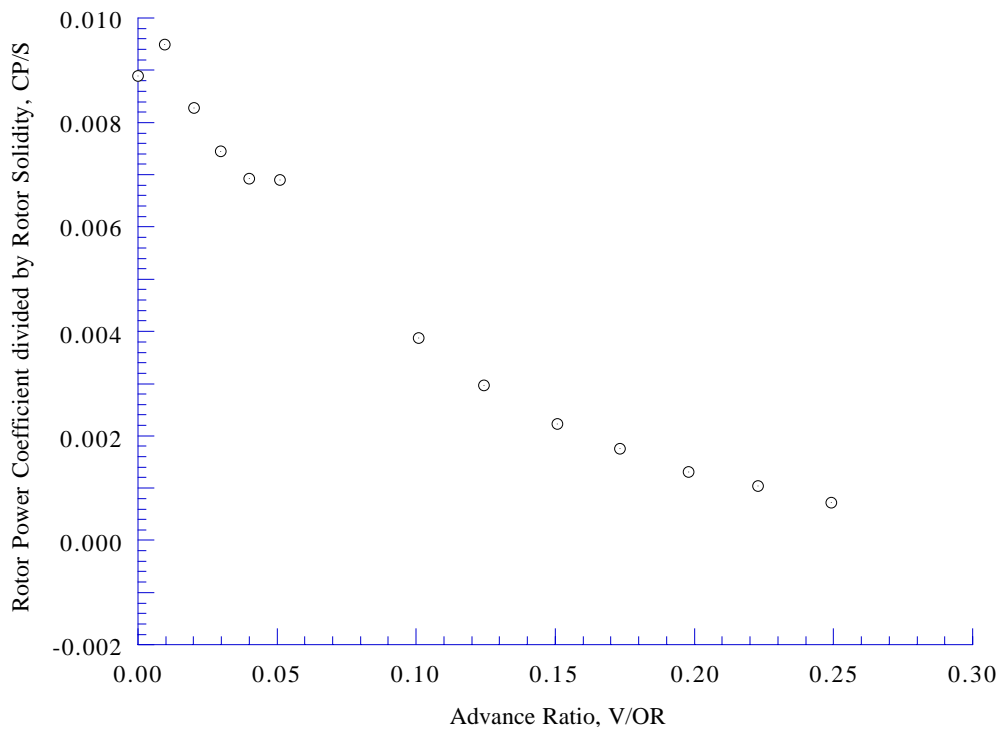


Figure 19(f). Rotor power coefficient as a function of advance ratio, $\alpha_S = 5 \text{ deg}$, $C_T/\sigma = 0.100$.

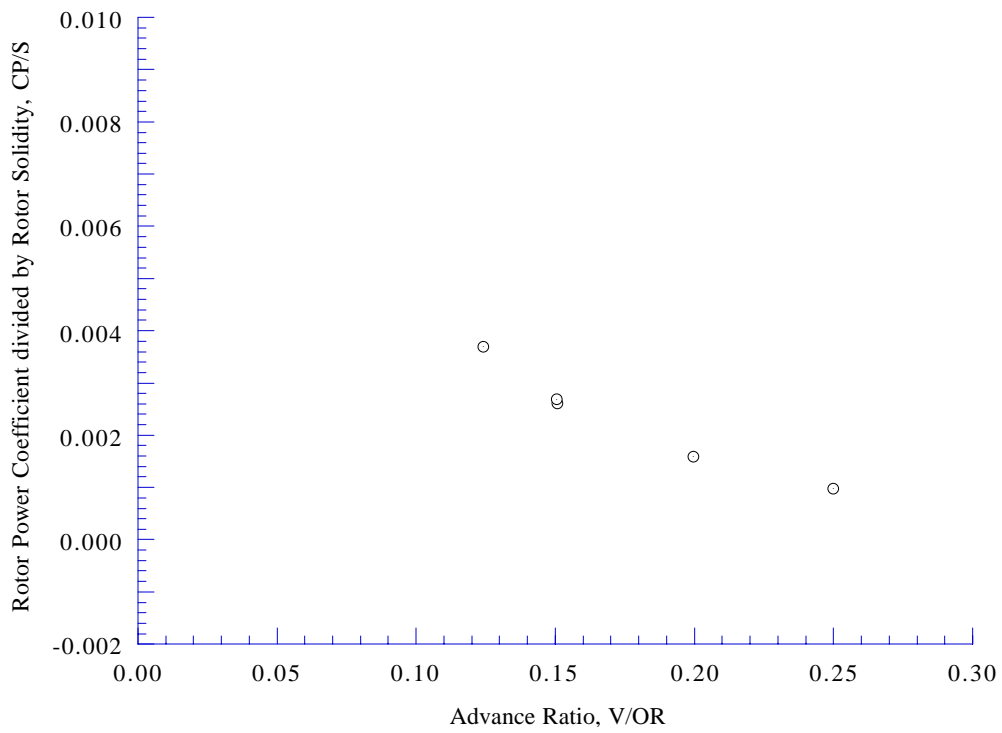


Figure 19(g). Rotor power coefficient as a function of advance ratio, $\alpha_S = 5 \text{ deg}$, $C_T/\sigma = 0.110$.

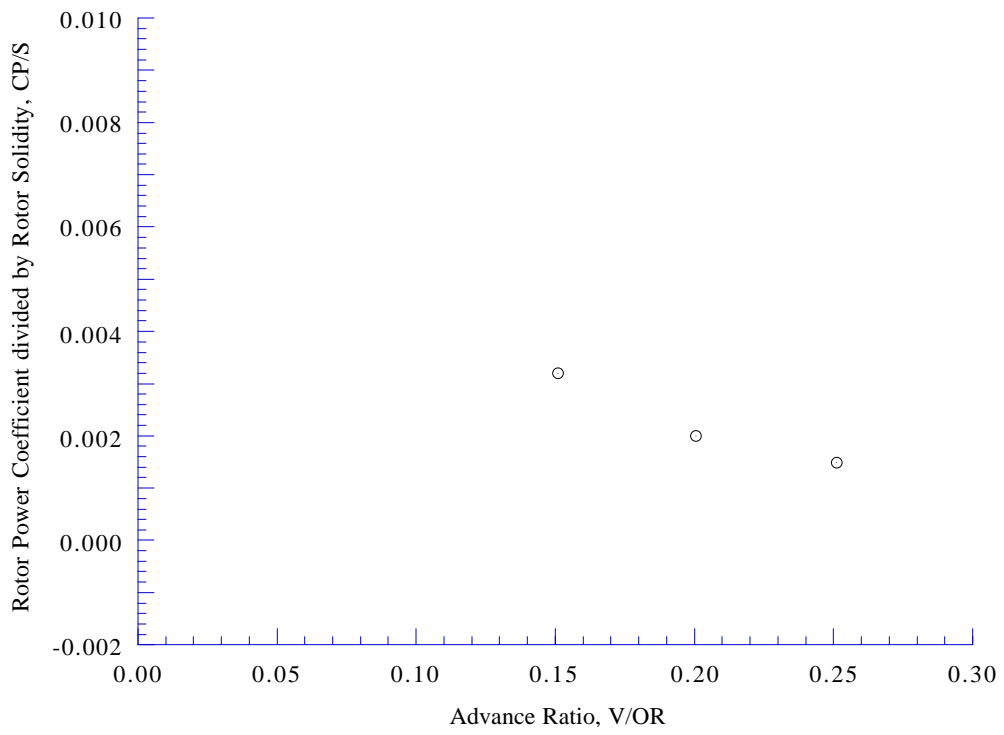


Figure 19(h). Rotor power coefficient as a function of advance ratio, $\alpha_S = 5 \text{ deg}$, $C_T/\sigma = 0.120$.

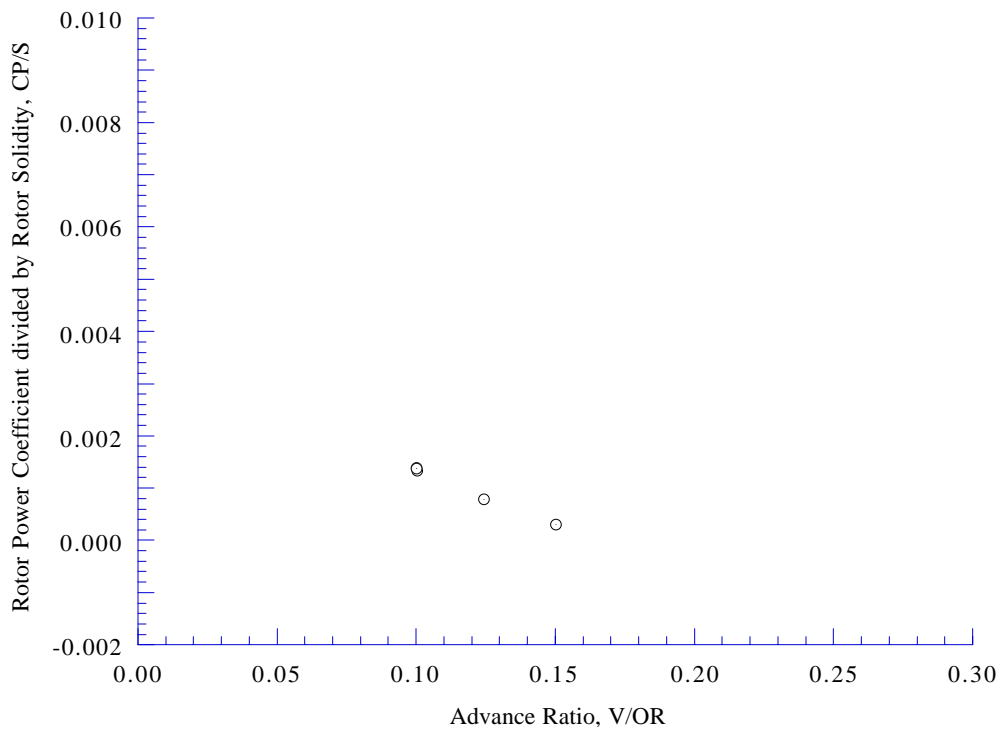


Figure 20(a). Rotor power coefficient as a function of advance ratio, $\alpha_S = 10 \text{ deg}$, $C_T/\sigma = 0.070$.

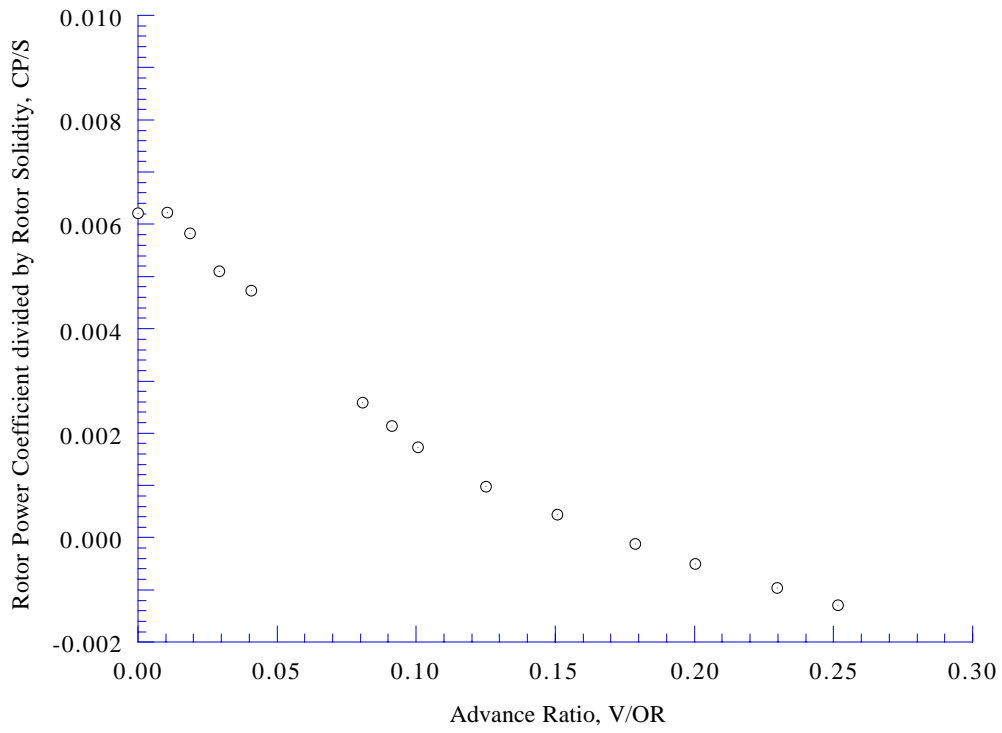


Figure 20(b). Rotor power coefficient as a function of advance ratio, $\alpha_S = 10 \text{ deg}$, $C_T/\sigma = 0.080$.

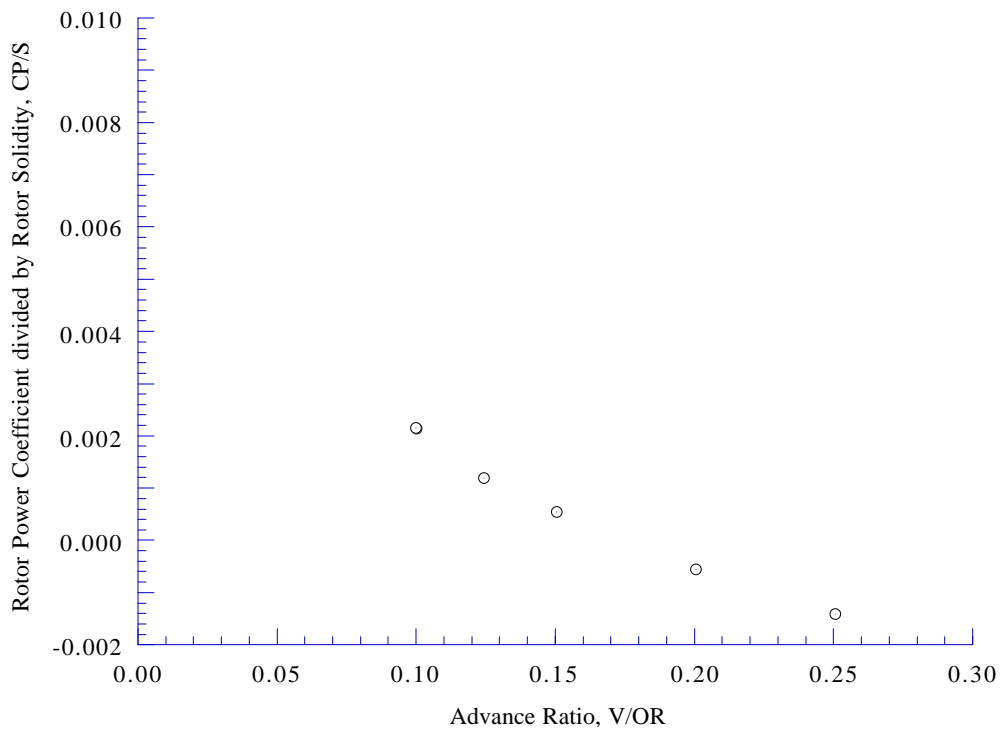


Figure 20(c). Rotor power coefficient as a function of advance ratio, $\alpha_S = 10 \text{ deg}$, $C_T/\sigma = 0.090$.

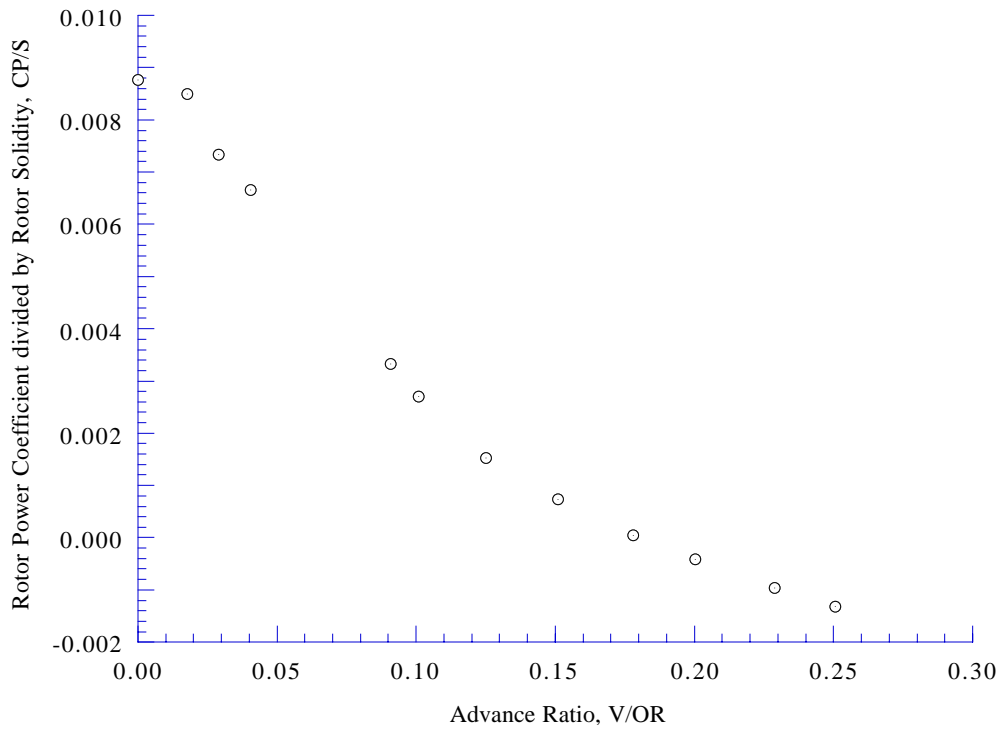


Figure 20(d). Rotor power coefficient as a function of advance ratio, $\alpha_S = 10 \text{ deg}$, $C_T/\sigma = 0.100$.

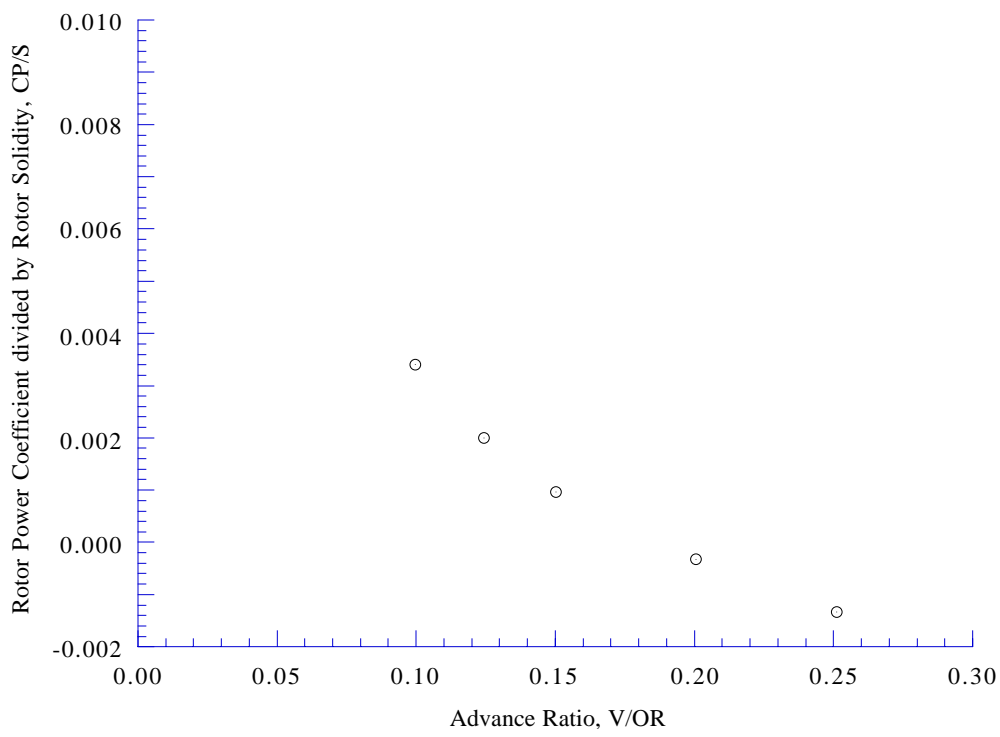


Figure 20(e). Rotor power coefficient as a function of advance ratio, $\alpha_S = 10$ deg, $C_T/\sigma = 0.110$.

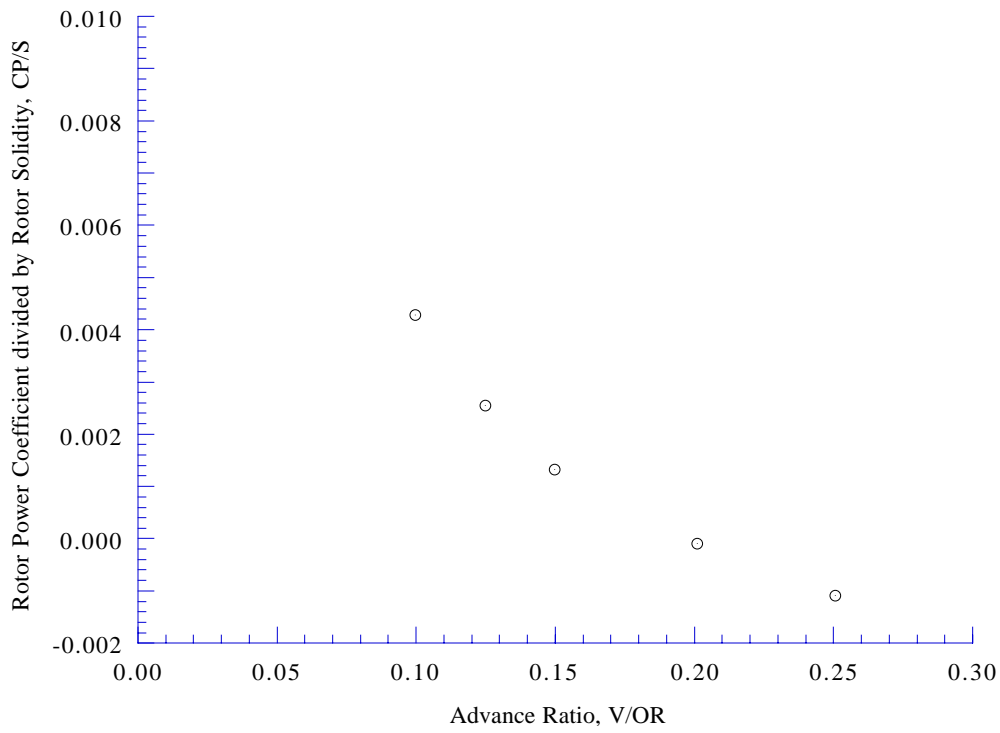


Figure 20(f). Rotor power coefficient as a function of advance ratio, $\alpha_S = 10$ deg, $C_T/\sigma = 0.120$.

REPORT DOCUMENTATION PAGE

Form Approved
OMB No. 0704-0188

Public reporting burden for this collection of information is estimated to average 1 hour per response, including the time for reviewing instructions, searching existing data sources, gathering and maintaining the data needed, and completing and reviewing the collection of information. Send comments regarding this burden estimate or any other aspect of this collection of information, including suggestions for reducing this burden, to Washington Headquarters Services, Directorate for Information Operations and Reports, 1215 Jefferson Davis Highway, Suite 1204, Arlington, VA 22202-4302, and to the Office of Management and Budget, Paperwork Reduction Project (0704-0188), Washington, DC 20503.

1. AGENCY USE ONLY (Leave blank)	2. REPORT DATE	3. REPORT TYPE AND DATES COVERED	
	April 1996	Technical Memorandum	
4. TITLE AND SUBTITLE		5. FUNDING NUMBERS	
Full-Scale S-76 Rotor Performance and Loads at Low Speeds in the NASA Ames 80- by 120-Foot Wind Tunnel Volume 2*		505-59-36	
6. AUTHOR(S)			
Patrick M. Shinoda			
7. PERFORMING ORGANIZATION NAME(S) AND ADDRESS(ES)		8. PERFORMING ORGANIZATION REPORT NUMBER	
Ames Research Center Moffett Field, CA 94035-1000		A-960974	
9. SPONSORING/MONITORING AGENCY NAME(S) AND ADDRESS(ES)		10. SPONSORING/MONITORING AGENCY REPORT NUMBER	
National Aeronautics and Space Administration Washington, DC 20546-0001		NASA TM-110379	
11. SUPPLEMENTARY NOTES			
Point of Contact: Patrick M. Shinoda, Ames Research Center, MS T-12B, Moffett Field, CA 94035-1000; (415) 604-6732			
*Volume 1 contains the main text and Appendices A-C. Volume 2 contains Appendix D.			
12a. DISTRIBUTION/AVAILABILITY STATEMENT		12b. DISTRIBUTION CODE	
Unclassified — Unlimited Subject Category 02			
13. ABSTRACT (Maximum 200 words)			
<p>A full-scale helicopter rotor test was conducted in the NASA Ames 80- by 120-Foot Wind Tunnel with a four-bladed S-76 rotor system. Rotor performance and loads data were obtained over a wide range of rotor shaft angles-of-attack and thrust conditions at tunnel speeds ranging from 0 to 100 kt. The primary objectives of this test were (1) to acquire forward flight rotor performance and loads data for comparison with analytical results; (2) to acquire S-76 forward flight rotor performance data in the 80- by 120-Foot Wind Tunnel to compare with existing full-scale 40- by 80-Foot Wind Tunnel test data that were acquired in 1977; (3) to evaluate the acoustic capability of the 80- by 120-Foot Wind Tunnel for acquiring blade vortex interaction (BVI) noise in the low speed range and compare BVI noise with in-flight test data; and (4) to evaluate the capability of the 80- by 120-Foot Wind Tunnel test section as a hover facility. The secondary objectives were (1) to evaluate rotor inflow and wake effects (variations in tunnel speed, shaft angle, and thrust condition) on wind tunnel test section wall and floor pressures; (2) to establish the criteria for the definition of flow breakdown (condition where wall corrections are no longer valid) for this size rotor and wind tunnel cross-sectional area; and (3) to evaluate the wide-field shadowgraph technique for visualizing full-scale rotor wakes. This data base of rotor performance and loads can be used for analytical and experimental comparison studies for full-scale, four-bladed, fully articulated rotor systems. Rotor performance and structural loads data are presented in this report.</p>			
14. SUBJECT TERMS		15. NUMBER OF PAGES	
Helicopter, Rotor performance, Rotor dynamics		939	
		16. PRICE CODE	
		A99	
17. SECURITY CLASSIFICATION OF REPORT	18. SECURITY CLASSIFICATION OF THIS PAGE	19. SECURITY CLASSIFICATION OF ABSTRACT	20. LIMITATION OF ABSTRACT
Unclassified	Unclassified		